

Transition-metal complexes of terpyridine ligands with hydroquinone or quinone substituents ‡

Gregory D. Storrer, Stephen B. Colbran *† and Donald C. Craig

School of Chemistry, University of New South Wales, Sydney, NSW 2052, Australia

The new ligands 4'-(2,5-dimethoxyphenyl)- (L¹), 4'-(2,5-hydroxyphenyl)- (L²) and 4'-(1,4-benzoquinonyl)-2,2':6',2''-terpyridine (L³) and a range of their transition-metal complexes have been prepared. The crystal and molecular structures of L¹ and [CuL¹][PF₆]₂ have been determined. Model reactions showed that the complexes [ML₂]ⁿ⁺ can be derivatized with suitable organic reagents, suggesting they may be incorporated into multi-component architectures using either ester or ether linkages. The chromophoric, magnetic and electrochemical properties of the complexes vary with transition metal and 4' substituent. The hydroquinonyl-substituted [ML₂]²⁺ and the quinonyl-substituted [ML₃]²⁺ complexes can be electrochemically interconverted in the presence of weak acid and switching between hydroquinonyl and quinonyl 4' substituents can significantly perturb physical properties of the bis(terpyridyl) transition-metal centre(s).

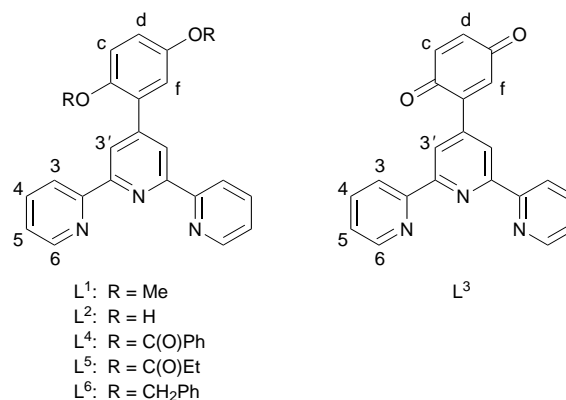
Multicomponent systems comprised covalently linked redox centres have attracted much recent attention.^{1–4} For example, bis(terpyridyl) transition-metal complexes,⁵ which display a diverse range of magnetic,^{5,6} photophysical^{2,4,7} and electrochemical^{3,5,8} properties, have recently found use as the electroactive or chromophoric centres in 'electron-reservoir' or 'photochemical' devices.^{2–4} Likewise, covalent supramolecular systems incorporating *p*-quinones as electron-transfer acceptors are the subject of intense current study,^{9–11} largely because electron-transfer reactions of *p*-quinones and *p*-hydroquinones play a pivotal role in biological processes, particularly photosynthesis and respiration.^{12,13} In these systems the properties of the transition-metal centre are often strongly perturbed by the electrochemically interconvertible *p*-quinone or *p*-hydroquinone groups.^{9–11} Interesting chemistry is therefore suggested for bis(terpyridyl) transition-metal systems with *p*-quinone or *p*-hydroquinone substituents. Ward and co-workers^{3a,b} have prepared some related bis(terpyridyl)ruthenium(II) complexes with catechol (*o*-hydroquinone) substituents and have shown that these substituents can co-ordinate to metal ions to give novel multicomponent assemblies. Herein we report transition-metal complexes of *p*-quinonyl- or *p*-hydroquinonyl-substituted terpyridyl ligands,¹⁴ including model reactions to test the suitability of these as starting materials for building multi-component assemblies and an example of using the *p*-quinone–*p*-hydroquinone couple to switch the physical properties exhibited by a bis(terpyridyl) transition-metal centre.

Results and Discussion

Synthetic studies

Ligand preparations. The entry point to the three new terpyridyl ligands, L¹–L³, was the synthesis of the 2,5-dimethoxyphenyl-substituted ligand, L¹. It was obtained by two routes: direct condensation¹⁵ of 2 equivalents of 2-acetylpyridine with 2,5-dimethoxybenzaldehyde in ammonium acetate–acetamide gave L¹, a pale yellow solid in 40% yield, whereas the two-step

synthesis,¹⁶ base-catalysed condensation of 2 equivalents of 2-acetylpyridine with 2,5-dimethoxybenzaldehyde to 3-(2,5-dimethoxyphenyl)-1,5-bis(2-pyridyl)pentane-1,5-dione (25% yield) followed by ring closure with ammonium acetate in air (75% yield), produced L¹ (19% overall yield). The direct route is more efficient in both time required and overall yield. Deprotection of L¹ with concentrated hydrobromic acid heated at reflux, followed by neutralization of the solution with sodium hydrogencarbonate afforded the hydroquinonyl ligand L² as light yellow crystals in 70% yield. Direct oxidation of the pendant hydroquinone in L² with 2,3-dichloro-5,6-dicyanobenzoquinone (ddq) followed by recrystallization from methanol gave quinonyl ligand L³, a light yellow powder in 55% yield.



Preparation of complexes. Homoleptic bis(terpyridyl) transition-metal complexes, [ML₂]²⁺ (L = L¹ or L²; M = Co, Cu, Mn, Ni or Zn), were obtained as their hexafluorophosphate salts in 65–85% yield from reactions of 2 equivalents of the ligand with the metal halide or metal acetate salt in methanol heated at reflux followed by metathesis with [NH₄][PF₆]. The homoleptic iron complexes, [FeL₂][BF₄]₂, were prepared directly from the ligand and [Fe(H₂O)₆][BF₄]₂ in methanol heated at reflux and the homoleptic ruthenium complexes [RuL₂][PF₆]₂ (L = L¹ or L²) were obtained from RuCl₃·*n*H₂O (40% Ru) or [Ru(dmsO)₄Cl₂] with 2 equivalents of the ligand in boiling ethanol or ethane-1,2-diol, respectively, followed by chromatography [silica support; acetonitrile–water–saturated aqueous KNO₃ (20:2:1) as eluent] and metathesis with [NH₄][PF₆]. Yields were in the range 55–90%. Reactions of 1 equivalent of L¹ and L² with [Ru(terpy)Cl₃] in aqueous ethanol at reflux in the

† E-Mail: S.Colbran@unsw.edu.au

‡ Supplementary data available: elemental analysis and spectroscopic data for the complexes. For direct electronic access see <http://www.rsc.org/suppdata/dt/1998/1351/>, otherwise available from BLDSC (No. SUP 57353, 5 pp.) or the RSC Library. See Instructions for Authors, 1998, Issue 1 (<http://www.rsc.org/dalton>).

Non-SI unit employed: μ_B ≈ 9.27 × 10^{–24} J T^{–1}.

presence of an excess of triethylamine, followed by metathesis with $[\text{NH}_4][\text{PF}_6]$, afforded the heteroleptic ruthenium complexes $[\text{Ru}(\text{terpy})\text{L}][\text{PF}_6]_2$ ($\text{L} = \text{L}^1$ or L^2). The rhodium(III) complexes, $[\text{RhL}_2][\text{PF}_6]_3$ ($\text{L} = \text{L}^1$ or L^2), were prepared by heating 2 equivalents of the appropriate ligand and RhCl_3 in ethanol containing *N*-ethylmorpholine.

The complexes of the hydroquinonyl-substituted ligand L^2 , $[\text{ML}_2]^{2+}$ ($\text{M} = \text{Co}, \text{Cu}, \text{Fe}, \text{Mn}, \text{Ni}, \text{Ru}$ or Zn), $[\text{Ru}(\text{terpy})\text{L}^2]^{2+}$ and $[\text{RhL}^2]^{3+}$, were also prepared by heating the corresponding complex of L^1 in 48% hydrobromic acid, followed by neutralization with NaHCO_3 , and recrystallization from methanol containing $[\text{NH}_4][\text{PF}_6]$. Yields were high, typically better than 85%.

The quinonyl-substituted complexes, $[\text{ML}_3]^{2+}$ ($\text{M} = \text{Co}, \text{Cu}, \text{Fe}, \text{Mn}, \text{Ni}, \text{Ru}$ or Zn), $[\text{Ru}(\text{terpy})\text{L}^3]^{2+}$ and $[\text{RhL}^3]^{3+}$, were prepared by addition of a slight excess ($\approx 5\%$) of ddq to an acetone solution of the analogous hydroquinonyl-substituted complex. Recrystallization from either acetone or methanol afforded the product complexes in better than 90% yield. Attempts to prepare $[\text{RuL}^3]^{2+}$ from the reaction of $[\text{Ru}(\text{dms})_4\text{Cl}_2]$ with L^3 (2.1 equivalents) gave a 3:1 mixture of $[\text{RuL}^3]^{2+}$ and $[\text{RuL}^2]^{2+}$ which could not be separated by fractional crystallization or chromatography; $[\text{RuL}^3]^{2+}$ was reduced to $[\text{RuL}^2]^{2+}$ by silica or gel permeation (Sephadex LH-120) supports.

Model oligomerization/polymerization reactions

(i) **Anodic electropolymerization of $[\text{RuL}_2]^{2+}$.** Electron-rich, methoxy-substituted arenes undergo anodic electropolymerization *via* coupling of electrochemically generated radical cations to afford polyarenes.¹⁷ It seemed possible that the $[\text{RuL}_2]^{2+}$ ion might also be polymerized under similar conditions to afford a 'string-of-pearls' type of co-ordination polymer held together by linked pairs of dimethoxyphenyl groups. Anodic electropolymerizations of $[\text{RuL}_2][\text{PF}_6]_2$ were attempted at platinum electrodes either by poisoning the electrode potential positive of that for oxidation of the dimethoxyphenyl groups (see below) or by repeatedly scanning the potential through this oxidation process. The medium used was acetonitrile or dichloromethane, containing 0.1 M tetrabutylammonium hexafluorophosphate, and both with and without trifluoroacetic acid containing 10% trifluoroacetic anhydride.¹⁷ No electropolymerization was observed. In contrast $[\text{Ru}(\text{o-dmptpy})_2]^{2+}$ [*o-dmptpy* = 4'-(3,4-dimethoxyphenyl)-2,2':6',2''-terpyridine] is readily electropolymerized.^{3b} The substitution of the methoxy groups in $[\text{Ru}(\text{o-dmptpy})_2]^{2+}$ and $[\text{RuL}_2]^{2+}$ is clearly critical with the *p*-dimethoxyphenyl substituents being insufficiently activated for anodic polymerization to take place.

(ii) **Ester and ether derivatives of $[\text{RuL}_2]^{2+}$ and $[\text{Ru}(\text{terpy})\text{L}^2]^{2+}$.** Polyesters are typically prepared by reactions of diacid halides, dicarboxylic acids or dicarboxylic acid anhydrides with organic dihydroxy compounds and reactions of organic dihalides with organic dihydroxy compounds yield polyethers.¹⁸ Hydroquinones are extensively used as the dihydroxy monomers in the manufacture of many polyesters and polyethers.¹⁸ The following model reactions were carried out to ascertain whether ester or ether derivatization reactions on complexes of hydroquinonyl-substituted L^2 were efficient.

Treatment of $[\text{RuL}_2]^{2+}$ and $[\text{Ru}(\text{terpy})\text{L}^2]^{2+}$ with a slight excess of either benzoyl chloride or propionyl chloride in acetonitrile-pyridine solution produced the new derivatized complexes $[\text{RuL}_2]^{2+}$ ($\text{L} = \text{L}^4$ or L^5) and $[\text{Ru}(\text{terpy})\text{L}^2]^{2+}$ ($\text{L} = \text{L}^4$ or L^5). The reactions were clean (¹H NMR spectra of the reaction mixtures suggest crude yields are above 90%), but the flash chromatography on silica and recrystallization steps necessary to produce pure products combine dramatically to reduce the overall yields to about 40–60%. Benzyl bromide and potassium carbonate in acetone converted $[\text{RuL}_2]^{2+}$ and $[\text{Ru}(\text{terpy})\text{L}^2]^{2+}$

into $[\text{RuL}_2]^{2+}$ and $[\text{Ru}(\text{terpy})\text{L}^2]^{2+}$, respectively. The NMR spectra suggested near-quantitative crude yields for these conversions, but, again, the purification procedures lead to only 55–60% overall yield of pure product.

We conclude that complexes of L^2 will be useful monomers for constructing multicomponent or polymeric inorganic systems held together by ester or ether linkages.^{3c-i} In this regard, we note recent reports by Constable and co-workers detailing ether-linked bis(terpyridyl)ruthenium(II) oligomers built up from preformed monomeric precursors.^{2e,3c,d} We also suggest that if high yields of ester- or ether-linked multicomponent systems are to be obtained from $[\text{ML}_2]^{n+}$ precursors, then chromatography steps should be avoided where possible (per-haps limited to the purification of the final targeted system).

(iii) **Reactions of L^3 and $[\text{Ru}(\text{terpy})\text{L}^3]^{2+}$ with aniline.** Amines, including anilines, undergo successive Michael addition and reoxidation reactions with *p*-quinones to afford diaminoquinones.¹⁹ With diamines, polyquinonylamines are formed with interesting properties such as electrical conductivity and the ability to displace water from wet, rusty iron surfaces.²⁰ These reactions suggested interesting quinonylamine-linked oligomers and polymers might be directly available from reactions of L^3 and its complexes with amines. As a test, a series of reactions of either L^3 or $[\text{Ru}(\text{terpy})\text{L}^3]^{2+}$ with an excess of aniline in a range of solvents (acetonitrile, chloroform, methanol, ethanol and dilute acetic acid) and conditions (either stirring at room temperature or heating to reflux) were attempted, all with the same result: no reaction was observed. The result is somewhat surprising. It suggests that terpyridyl substitution renders the quinone group in L^3 inert to Michael addition by aniline and, furthermore, that co-ordination of L^3 to an electropositive metal centre does not activate the quinone group sufficiently for Michael addition (as might be expected from simple electrostatic arguments). We conclude, unfortunately, that quinonylamine-linked oligomers and polymers are not available from reactions of L^3 and its complexes with arylamines.

Characterization and properties

Tables of partial elemental analysis, electrospray mass spectral and ¹H and ¹³C NMR data for the ligands and complexes are given in SUP 57353. The elemental analyses were acceptable [given some hydration as is commonly observed for bis(terpyridyl) transition-metal salts^{3a,b,16,21}]. The NMR spectroscopic and TLC analysis independently confirmed the purity of the complexes. The NMR and electrospray mass spectral data of the complexes are unremarkable and fully consistent with the formulations given. In the infrared spectra complexes of L^1 showed arylether stretching bands at ≈ 1040 and 1020 cm^{-1} (*cf.* 1054 and 1042 cm^{-1} for L^1), those of L^2 exhibited broad O–H stretches centred at $\approx 3540 \text{ cm}^{-1}$ (*cf.* 3110 cm^{-1} for L^2), and those of L^3 revealed medium-strong quinonyl C=O stretching bands at $\approx 1660 \text{ cm}^{-1}$ (*cf.* 1665 cm^{-1} for L^3).

Crystal structures. Ligand L^1 crystallized from diethyl ether in the monoclinic space group *C2/c* with eight molecules in the unit cell. Selected bond length and angle data are presented in Table 1. The crystal structure comprises oblique columns of antiparallel, π -stacked molecules of L^1 running parallel to the diagonal bisecting the *a* and *c* axes. Within the oblique columns, the central pyridyl ring of each molecule of L^1 is π -stacked with that one adjacent L^1 molecule whereas the terminal terpyridyl rings are π -stacked with those of the other neighbouring L^1 molecule, Fig. 1. The average interplanar distance between the π -stacked terpyridyl rings is 3.5 Å. Pairs of dimethoxyphenyl substituents are also π -stacked, with an average interplanar distance of 3.6 Å, Fig. 1.

A view of the molecular structure of L^1 is presented in Fig. 2. Within the ligand the three pyridyl rings are approximately coplanar (torsional angles between the central and terminal

Table 1 Selected bond lengths (Å) and torsional angles (°) for L^1 with estimated standard deviations (e.s.d.s) in parentheses

N1–C1	1.327(3)	N3–C11	1.340(3)
C5–N1	1.332(2)	C8–C16	1.484(2)
C5–C6	1.480(3)	C17–O1	1.372(2)
C10–N2	1.344(2)	O1–C22	1.397(2)
N2–C6	1.341(2)	C20–O2	1.381(2)
C10–C11	1.485(2)	O2–C23	1.424(3)
C15–N3	1.335(3)		
N1–C5–C6–N2	–179.6(2)	N2–C10–C11–N3	–179.3(2)
C7–C8–C16–C17	51.6(2)	C7–C8–C16–C21	–129.7(2)
C9–C8–C16–C17	–131.5(2)	C9–C8–C16–C21	47.2(2)

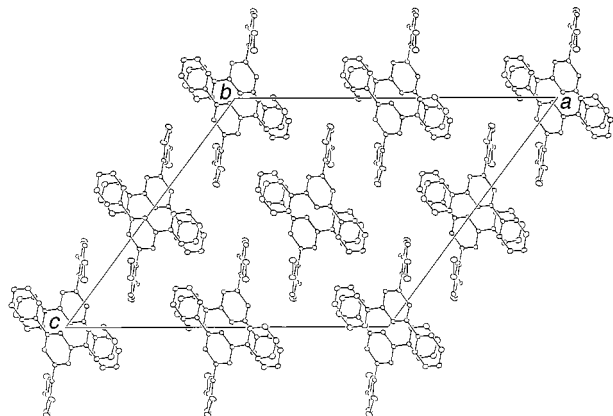


Fig. 1 Packing of molecules in the crystal structure of compound L^1 , viewed down the b axis

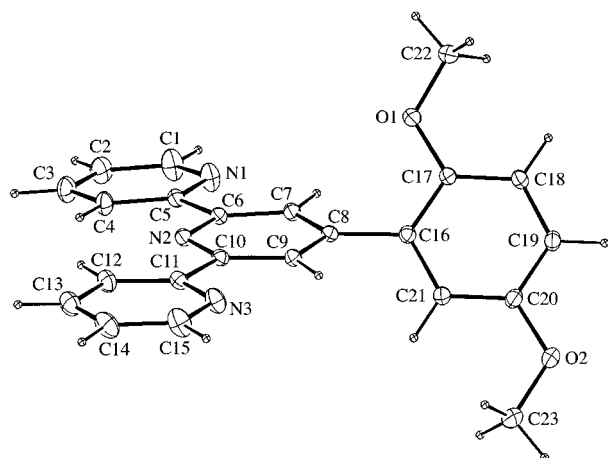


Fig. 2 An ORTEP²² plot of L^1 (20% thermal ellipsoids for non-hydrogen atoms)

pyridyl rings are in the range 0.1–1.3°) and adopt the expected transoid arrangement which minimizes interactions between nitrogen lone pairs. The C–C and C–N bond lengths within the aromatic rings are normal and average 1.373 ± 0.003 and 1.335 ± 0.003 Å, respectively. The three interannular C–C bond distances average 1.480 ± 0.003 Å, slightly longer than those reported for 4'-phenyl-2,2':6',2''-terpyridine (ptery) which average 1.439 ± 0.001 Å.¹⁶ Presumably as a result of intramolecular steric interactions, the dimethoxyphenyl substituent in L^1 is not coplanar with the terpyridyl moiety but is significantly twisted about the interannular bond, making an angle of 50.2° with the central pyridyl ring (for comparison, the corresponding interannular twist in ptery is 10.9°).¹⁶

Emerald green crystals of $[\text{CuL}^1_2][\text{PF}_6]_2 \cdot \text{MeOH}$ shown by crystallographic analysis to be $[\text{CuL}^1_2][\text{PF}_6]_2 \cdot \text{MeOH}$ (Table 2, Fig. 3), were obtained on diffusion of diethyl ether vapour into a solution of $[\text{CuL}^1_2][\text{PF}_6]_2$ in acetone–methanol (1:3). The

Table 2 Selected bond lengths (Å) and angles (°) for $[\text{CuL}^1_2][\text{PF}_6]_2 \cdot \text{MeOH}$ with e.s.d.s in parentheses

Cu–N1A	2.235(5)	Cu–N1B	2.127(6)
Cu–N2A	1.983(5)	Cu–N2B	1.957(5)
Cu–N3A	2.221(5)	Cu–N3B	2.132(6)
C5A–C6A	1.482(9)	C5B–C6B	1.459(9)
C8A–C16A	1.487(9)	C8B–C16B	1.490(9)
C10A–C11A	1.480(9)	C10B–C11B	1.505(9)
N1A–Cu–N2A	77.0(2)	N2A–Cu–N3B	104.4(2)
N1A–Cu–N3A	154.2(2)	N3A–Cu–N1B	97.3(2)
N1A–Cu–N1B	87.6(2)	N3A–Cu–N2B	105.2(2)
N1A–Cu–N2B	100.6(2)	N3A–Cu–N3B	87.8(2)
N1A–Cu–N3B	97.6(2)	N1B–Cu–N2B	79.2(2)
N2A–Cu–N3A	77.3(2)	N1B–Cu–N3B	156.7(2)
N2A–Cu–N1B	98.9(2)	N2B–Cu–N3B	77.5(2)
N2A–Cu–N2B	177.0(2)		

Table 3 Magnetic moments ($\pm 10\%$) measured using the Evans method in acetone solution at 294 K

Complex	μ/μ_B
$[\text{CoL}^1_2][\text{PF}_6]_2 \cdot \text{H}_2\text{O}$	3.84
$[\text{CoL}^2_2][\text{PF}_6]_2 \cdot 2\text{H}_2\text{O}$	3.52
$[\text{CoL}^3_2][\text{PF}_6]_2 \cdot 3\text{H}_2\text{O}$	2.73
$[\text{CuL}^1_2][\text{PF}_6]_2 \cdot \text{H}_2\text{O}$	2.34
$[\text{CuL}^2_2][\text{PF}_6]_2 \cdot \text{H}_2\text{O}$	2.63
$[\text{CuL}^3_2][\text{PF}_6]_2 \cdot 2\text{H}_2\text{O}$	2.27
$[\text{MnL}^1_2][\text{PF}_6]_2$	6.09
$[\text{MnL}^2_2][\text{PF}_6]_2 \cdot \text{H}_2\text{O}$	5.86
$[\text{MnL}^3_2][\text{PF}_6]_2 \cdot \text{H}_2\text{O}$	5.86
$[\text{NiL}^1_2][\text{PF}_6]_2 \cdot 2\text{H}_2\text{O}$	3.26
$[\text{NiL}^2_2][\text{PF}_6]_2 \cdot 2\text{H}_2\text{O}$	3.16
$[\text{NiL}^3_2][\text{PF}_6]_2 \cdot \text{H}_2\text{O}$	3.04

only noteworthy intermolecular contact in the crystal structure is face-to-face π stacking at a distance of ≈ 3.7 Å between the dimethoxyphenyl substituents of cations in adjacent unit cells. The copper(II) ion displays the expected orthorhombic distortion from octahedral symmetry, observed in $[\text{Cu}(\text{terpy})_2][\text{NO}_3]_2$ ²³ and in more closely related $[\text{Cu}(\text{anterpy})_2][\text{BF}_4]_2$ [anterpy = 4'-(4-anilino)-2,2':6',2''-terpyridine].^{3m} The Cu–N (terminal pyridyl ring) distances for the two ligands are significantly different, with those to ligand B [average 2.130(6) Å] shorter than those to ligand A [average 2.228(6) Å] while the two Cu–N (central pyridyl ring) distances are 1.983(5) (ligand A) and 1.957(5) Å (B). To accommodate the longer Cu–N (terminal terpyridyl ring) distances, the interannular bonds within the terpyridyl moiety of ligand A are significantly more twisted [e.g. torsional angles: N1A–C5A–C6A–N2A $-11.3(9)$ and N2A–C10A–C11A–N3A $-9.4(9)^\circ$] than in B [e.g. N1B–C5B–C6B–N2B $-6.0(8)$ and N2B–C10B–C11B–N3B $-3.0(8)^\circ$]. Interestingly, although the central pyridyl rings of the two terpyridyl ligands are oppositely aligned as expected [N2A–Cu–N2B $177.0(2)^\circ$], the angle between the planes of these rings is 78° revealing a moderate twist from the expected orthogonal arrangement for the two terpyridyl ligands. The inequivalence of the two terpyridyl ligands is also revealed by the angles between the central pyridyl and dimethoxyphenyl rings within each ligand [41° for ligand A and 37° for B compared with 50° in the free terpyridine (see above)].

Magnetic properties. Table 3 lists magnetic moment data for the paramagnetic complexes in acetone solution obtained by ¹H NMR spectroscopy using the Evans method.²⁴ Owing to the tendency of the complexes to crystallize from different recrystallizations with varying amounts of water or other solvent, all measurements were made on samples characterized by elemental analysis. The reproducibility of the results was $\pm 10\%$. The manganese and nickel complexes exhibit magnetic moments typical of octahedral, high-spin d^5 manganese(II) and

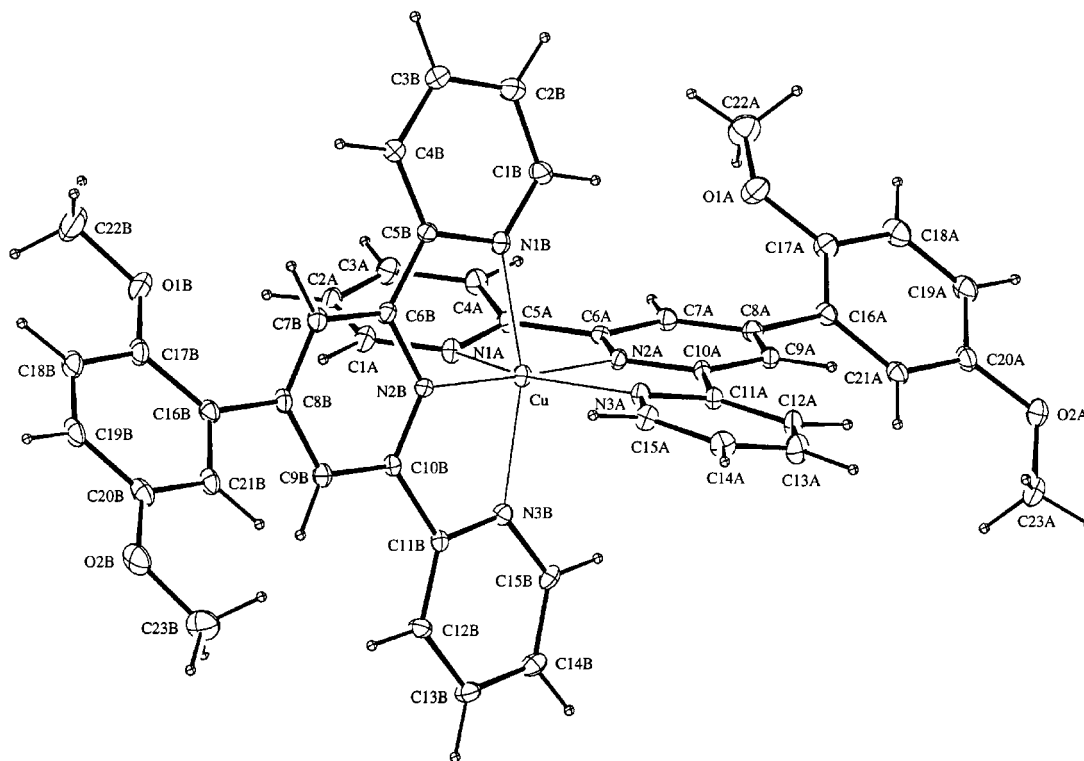


Fig. 3 An ORTEP plot of the cation $[\text{CuL}^1]^{2+}$ (20% thermal ellipsoids for non-hydrogen atoms)

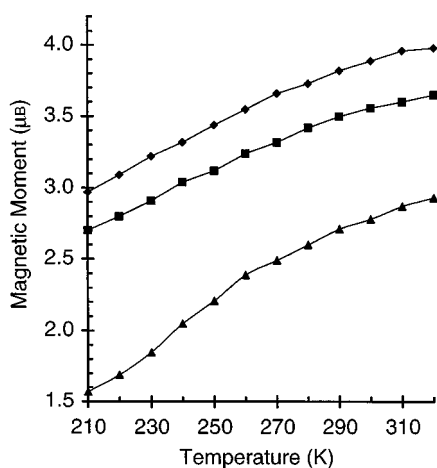


Fig. 4 Temperature-dependent magnetic moment data for $[\text{CoL}^1]^{2+}$ ($[\text{PF}_6]_2 \cdot \text{H}_2\text{O}$ (◆)), $[\text{CoL}^2]^{2+}$ ($[\text{PF}_6]_2 \cdot 2\text{H}_2\text{O}$ (■)) and $[\text{CoL}^3]^{2+}$ ($[\text{PF}_6]_2 \cdot 3\text{H}_2\text{O}$ (▲)) in acetone solution

d^8 nickel(II) species respectively. The values for $[\text{CuL}_2][\text{PF}_6]_2$ ($L = L^1-L^3$) are slightly higher than generally expected for distorted octahedral d^9 copper(II) complexes (typically 1.8–2.2 μ_B). Except for the cobalt(II) complexes of L^1-L^3 , the magnetic moments for the three complexes of a particular metal ion show little variation as the 4' substituents are changed.

Fig. 4 presents the magnetic moment data for the cobalt(II) complexes in acetone solution over 210–320 K. The magnetic moments are temperature dependent and indicative of incomplete, continuous (*i.e.* gradual) spin transitions between low-spin (2E_g) and high-spin (4T_g) states, as expected for d^7 bis(terpyridyl)cobalt(II) complexes. Spin-crossover behaviour in crystalline bis(terpyridyl)cobalt(II) salts is dictated by lattice forces and is critically dependent on the degree of hydration {this accounts for the reports of six structural analyses of $[\text{Co}(\text{terpy})_2]^{2+}$ salts^{21, 5,6}. The spin-crossover behaviour exhibited by a solution containing a bis(terpyridyl)cobalt(II) cation, however, should be independent of any lattice solvent in the salt dissolved to make the solution. At a given temperature

the magnetic moments of the $[\text{CoL}_2]^{2+}$ ($L = L^1$ or L^2) complexes are within experimental error of each other. The magnetic moments for $[\text{CoL}^3]^{2+}$ are significantly lower (by ≈ 1.4 – $0.8 \mu_B$ depending on temperature, see Fig. 4) indicating more of the low-spin complex at a particular temperature and suggesting that L^3 exerts a stronger ligand field than does L^1 or L^2 . This is consistent with the σ -donor properties of the terpyridyl ligands varying little with the 4' substituents and with the dimethoxyphenyl and hydroquinonyl groups acting as π -donor substituents and the quinone groups acting as π -acceptor substituents. The results demonstrate that the magnetic properties of a bis(terpyridyl)cobalt(II) complex can be switched by changing the state-of-charge of redox-active 4' substituents, in this case switching from hydroquinone to quinone substituents. Possible molecular electronics applications, for example as memory elements that are addressed electrochemically and read magnetically, can be envisaged.²⁵

We also obtained ^1H NMR spectra of the paramagnetic cobalt(II) complexes. The spectrum of $[\text{CoL}^1]^{2+}$ shows nine resonances, all significantly paramagnetically shifted, Fig. 5(a). The five broad resonances at lowest field, A–E, are assigned to the terpy protons of the $[\text{Co}(\text{terpy})_2]^{2+}$ core and correspond closely in position and appearance to those found in related bis(terpyridyl)cobalt(II) complexes.^{3k,o-q} The remaining peaks are attributed to the dimethoxyphenyl groups: the δ 9.8 resonance is a doublet, coupled to the δ 9.0 signal, and arises from either H^4 or H^5 ; the δ 9.0 signal arises from the overlap of a singlet for H^6 and a doublet for either H^3 or H^4 respectively; the two remaining peaks at δ 5.5 and 5.8 are the methoxy resonances. In the spectrum of $[\text{CoL}^2]^{2+}$, Fig. 5(b), there are five resonances in addition to A–E for the $[\text{Co}(\text{terpy})_2]^{2+}$ core. Provided the two hydroquinonyl groups are equivalent, five resonances for the hydroquinonyl protons are expected. Definite assignments have not been made but likely assignments are: hydroxy protons at δ 12.1 and 10.1, H^6 the singlet at δ 9.1, and H^3 and H^4 the doublets at δ 9.6 and 8.8.

In contrast with the spectra of $[\text{CoL}_2]^{2+}$ ($L = L^1$ or L^2), peaks A–E for the $[\text{Co}(\text{terpy})_2]^{2+}$ core are not observed in the spectrum of $[\text{CoL}^3]^{2+}$, Fig. 5(c). Rather seven resonances are observed between δ 10 and 7. Two are doublets (at δ 7.4 and

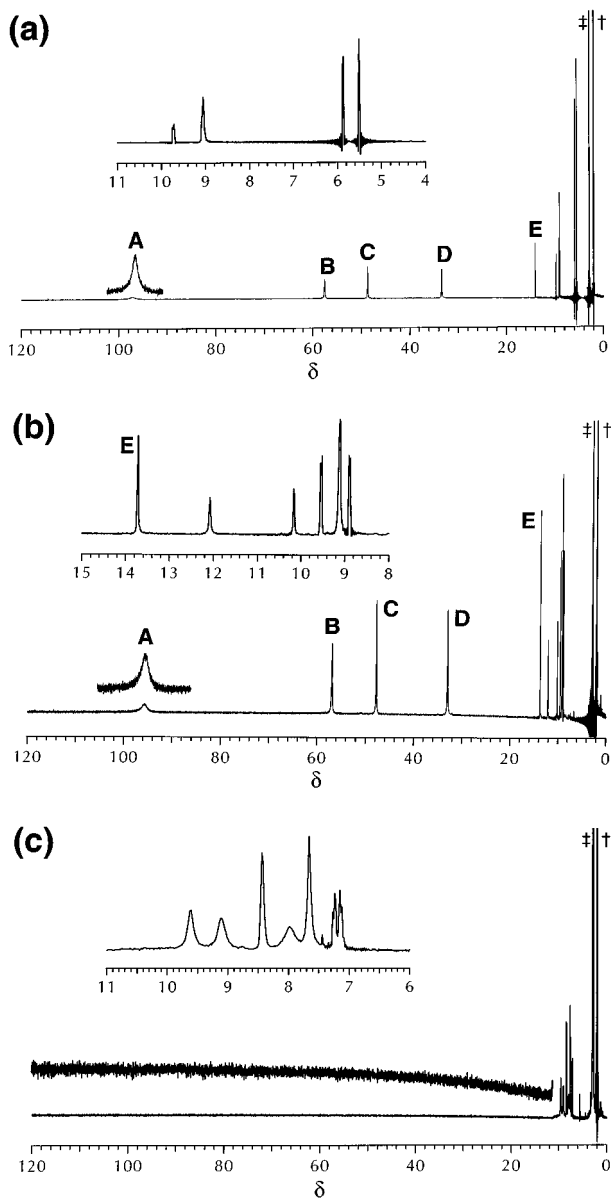


Fig. 5 The 300 MHz ^1H NMR spectra of the cobalt complexes in $[\text{D}_6]\text{acetone}$ solution at 298 K: (a) $[\text{CoL}_2][\text{PF}_6]_2 \cdot \text{H}_2\text{O}$, (b) $[\text{CoL}_2][\text{PF}_6]_2 \cdot 2\text{H}_2\text{O}$ and (c) $[\text{CoL}_3][\text{PF}_6]_2 \cdot 3\text{H}_2\text{O}$. Peaks for water (\ddagger) and residue protio-solvent (\dagger) are marked

7.3) and may be assigned as the H^3 and H^4 resonances of the quinonyl groups. The remaining peaks are broad and are likely the five proton resonances of the $[\text{Co}(\text{terpy})_2]^{2+}$ core. The resonance for H^6 of the quinonyl groups probably lies under one of these peaks. The large shifts in resonance frequencies of paramagnetic transition-metal complexes are made up of two components, the electron-nucleus dipolar interaction and the (usually much larger) Fermi contact shift, which both scale as $S(S+1)$ where S is the electron spin quantum number.²⁶ The paramagnetic shifts therefore indicate a higher population ratio of low-spin ($S = \frac{1}{2}$) states: high-spin ($S = \frac{3}{2}$) states for $[\text{CoL}_3]^{2+}$ than for $[\text{CoL}_2]^{2+}$ ($L = \text{L}^1$ or L^2), consistent with the lower magnetic moment for $[\text{CoL}_3]^{2+}$ in acetone solution (see above).

Absorption spectroscopy. The UV/VIS spectra of ligands L^1 – L^3 reveal a collection of intense bands below 400 nm which are attributed to terpyridyl-centred $\pi \rightarrow \pi^*$ transitions by com-

parison with the spectrum of pterpy.¹⁶ Quinonyl-substituted L^3 also exhibited a band at 470 nm ($\epsilon \approx 500 \text{ M}^{-1} \text{ cm}^{-1}$) which is associated with the quinonyl moiety but has not been assigned [for comparison, 1,4-benzoquinone shows a spin-allowed $\pi \rightarrow \pi^*$ transition at 242 (20 300), a spin-forbidden $\pi \rightarrow \pi^*$ transition at 289 (285) and a spin-forbidden $n \rightarrow \pi^*$ transition at 437 nm ($20 \text{ M}^{-1} \text{ cm}^{-1}$); the energies and intensities of the last two bands are very sensitive to substitution of the quinone ring²⁸].

Details of the electronic spectra of the complexes are summarized in Table 4. The complexes of Mn^{II} , Co^{II} , Ni^{II} , Cu^{II} and Zn^{II} show the same bands as those of the respective ligands but with greatly increased absorption coefficients (by 2–10 times). The weak bands in the visible region at ≈ 700 nm for the complexes of Co^{II} and Cu^{II} and at ≈ 800 nm for the nickel(II) complexes are also observed for the corresponding $[\text{M}(\text{terpy})_2]^{2+}$ complex and are attributed to d–d bands.⁵ Charge-transfer bands dominate the visible regions of the spectra of the complexes Fe^{II} , Ru^{II} , Co^{II} and Rh^{II} .^{2,4,7} Notably, the energies of the expected $d_{\pi}(\text{metal}) \rightarrow \pi^*(\text{terpy})$ metal-to-ligand charge transfer (MLCT) bands for the iron(II) (at ca. 565 nm) and the ruthenium(II) complexes (at ca. 490 nm) are all about that of the corresponding pterpy complex,^{4,7} suggesting that switching the aryl or quinone group in these complexes either has little effect on the metal centre or moves the metal d_{π} and ligand π^* orbital energies in concert. Interestingly, the $d_{\pi}(\text{Co}) \rightarrow \pi^*(\text{terpy})$ MLCT band at 503 nm in the visible spectrum of quinone-substituted $[\text{CoL}_3]^{2+}$ is significantly higher in energy than the corresponding bands for $[\text{CoL}_2]^{2+}$ ($L = \text{L}^1$, L^2 or pterpy) which are all at 514 nm. Quinone-substituted L^3 being the better π -acceptor ligand presumably slightly lowers the energy of the $d_{\pi}(\text{Co})$ orbitals in $[\text{CoL}_3]^{2+}$ thereby slightly increasing the MLCT band energy compared to those of the other cobalt(II) complexes. A slight increase in the ligand-field strength as a result of the lower $d_{\pi}(\text{Co})$ orbital energies in $[\text{CoL}_3]^{2+}$ also accounts for the different temperature dependence of the magnetism exhibited by this complex (see above). The rhodium(III) homoleptic complexes, $[\text{RhL}_2]^{3+}$ ($L = \text{L}^1$ – L^3), exhibit intense charge-transfer bands at 422, 449 and 446 nm, respectively, compared to $[\text{Rh}(\text{terpy})_2]^{3+}$ for which the lowest-energy band is at 356 nm.⁴

The chemically reversible *p*-quinone–*p*-hydroquinone couple has been used to switch the luminescence from poly(pyridyl)-ruthenium(II) centres with these groups as substituents on (*p*-hydroquinone)/off (*p*-quinone).¹¹ We wondered if the complexes $[\text{RuL}_2]^{2+}$ ($L = \text{L}^2$ or L^3) would exhibit the same electro-switchable behaviour and, therefore, recorded luminescent spectra of these complexes in fluid solution. Although many bis(terpyridyl)ruthenium(II) complexes are non-luminescent in fluid solution, acetonitrile solutions of 4'-aryl-substituted terpyridine (4'-R-terpy) complexes, $[\text{Ru}(4'\text{-R-terpy})_2]^{2+}$, in acetonitrile at 298 K typically exhibit very weak, broad luminescence bands in the visible region attributed to emission from the lowest-energy $^3\text{MLCT}$ excited state.^{4,7} Unfortunately, under the same conditions no luminescence was observed from the complexes $[\text{RuL}_2]^{2+}$ ($L = \text{L}^1$ – L^3).

Electrochemistry. The electrochemical responses of the ligands and all complexes were characterized by cyclic and differential pulse voltammetry and bulk coulometry experiments in acetonitrile–0.1 M $[\text{NBu}_4][\text{PF}_6]$.

Ligands. The cyclic voltammogram of L^1 shows a quasi-reversible oxidation of the dimethoxyphenyl moiety²⁹ at +0.95 V [$i_{\text{pc}}/i_{\text{pa}} = 0.56$, $\Delta E_{\text{p}} = 100$ mV vs. $\Delta E_{\text{p}}(\text{ferrocenium-ferrocene}) = 76$ mV]. Bulk electrolysis experiments revealed the oxidation to be a one-electron process. The cathodic peak at –2.54 V, with coupled peaks in the reverse scan at –2.16 and –1.62 V (the latter peak was small), is attributed to reduction of the terpyridyl centre. The irreversible nature of the reduction suggests that the terpyridyl radical anion is unstable. A broad

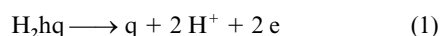
§ Although not attempted, it may be possible to deconvolute the contributions of the dipolar and contact shift terms to the paramagnetic shifts by comparison of the NMR spectral data of cobalt(II) complexes with those for their nickel(II) analogues.²⁷

Table 4 The UV/VIS spectroscopic data for the new complexes^a

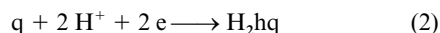
[CoL ¹][PF ₆] ₂	514 (2.8), 367 (12.0), 319 (37.4), 284 (69.1), 276 (sh, 60.2), 205 (113.6)
[CuL ¹][PF ₆] ₂	689 (0.075), ^b 372 (10.9), 339 (sh, 31.3), 327 (35.7), 285 (68.1), 278 (64.4), 269 (sh, 56.4), 226 (sh, 73), 205 (117.7)
[MnL ¹][PF ₆] ₂	364 (sh, 5.5), 336 (sh, 19.6), 325 (22.2), 284 (42.4), 278 (39.6), 231 (39.6), 202 (79.9)
[NiL ¹][PF ₆] ₂	796 (0.032), ^b 373 (9.7), 336 (16.2), 325 (28.7), 282 (62.7), 229 (sh, 31.2), 202 (70.2)
[ZnL ¹][PF ₆] ₂	372 (8.8), 336 (30.6), 326 (33.1), 284 (60.5), 278 (55.4), 231 (49.3), 202 (111.6)
[FeL ¹][BF ₄] ₂	564 (26.0), 361 (sh, 14.0), 322 (50.9), 284 (75.4), 277 (62.5), 202 (114)
[RhL ¹][PF ₆] ₃	422 (10.6), 357 (21.9), 339 (28.1), 326 (30.1), 295 (69.4), 243 (53.0)
[RuL ¹][PF ₆] ₂	489 (35.3), 310 (83.1), 282 (78.1), 276 (79.8), 203 (104.6)
[Ru(terpy)L ¹][PF ₆] ₂	482 (21.7), 309 (67.3), 282 (sh, 45), 273 (50.7), 201 (67.5)
[CoL ²][PF ₆] ₂	514 (4.3), 391 (13.9), 316 (47.8), 284 (82.7), 205 (126.1)
[CuL ²][PF ₆] ₂	655 (0.160), ^b 391 (8.8), 325 (31.1), 285 (56.2), 278 (sh, 50.6), 269 (sh, 42.5), 205 (89.5)
[MnL ²][PF ₆] ₂	377 (6.9), 325 (27.3), 285 (54.1), 278 (48.9), 230 (44.7), 204 (84.1)
[NiL ²][PF ₆] ₂	781 (0.065), ^b 388 (10.1), 335 (sh, 25.5), 323 (31.3), 283 (68.2), 206 (97.7)
[ZnL ²][PF ₆] ₂	387 (10.2), 334 (sh, 33.1), 325 (35.7), 285 (64.7), 278 (sh, 57.8), 230 (47.7), 203 (98.7)
[FeL ²][BF ₄] ₂	566 (24.7), 365 (sh, 13.2), 322 (44.7), 284 (78.7), 277 (sh, 51.8), 202 (103.4)
[RhL ²][PF ₆] ₃	449 (10.7), 355 (sh, 15.5), 338 (sh, 22.5), 295 (sh, 43.1), 286 (45.4), 241 (43.5)
[RuL ²][PF ₆] ₂	491 (37.1), 310 (92.2), 283 (83.0), 276 (78.2)
[Ru(terpy)L ²][PF ₆] ₂	483 (17.2), 309 (64.3), 273 (58.6)
[CoL ³][PF ₆] ₂	503 (5.0), 391 (16.2), 313 (38.7), 284 (67.4), 278 (sh, 61.1), 204 (112.5)
[CuL ³][PF ₆] ₂	680 (sh, 0.160), ^b 470 (sh, 6.0), 388 (10.1), 325 (33.2), 286 (60.3), 279 (sh, 60.0), 269 (sh, 50.4), 223 (sh, 76.6), 202 (107.1)
[MnL ³][PF ₆] ₂	458 (sh, 6.7), 381 (10.8), 333 (sh, 38.8), 323 (44.2), 285 (84.0), 277 (sh, 75.9), 233 (73.8), 203 (124.3)
[NiL ³][PF ₆] ₂	765 (sh, 0.095), 476 (sh, 4.5), 386 (12.5), 335 (sh, 32.1), 323 (39.1), 283 (81.1), 204 (120.8)
[ZnL ³][PF ₆] ₂	454 (sh, 5.4), 387 (8.8), 334 (sh, 30.6), 324 (34.2), 285 (61.3), 279 (sh, 54.6), 232 (49.6)
[FeL ³][BF ₄] ₂	567 (22.5), 365 (11.9), 322 (48.5), 284 (69.4), 277 (sh, 60.6), 202 (99.3)
[RhL ³][PF ₆] ₃	446 (13.1), 356 (27.9), 341 (33.0), 326 (32.0), 290 (61.4), 244 (62.7)
[RuL ³][PF ₆] ₂	491 (31.5), 309 (76.4), 282 (74.2), 276 (75.3)
[Ru(terpy)L ³][PF ₆] ₂	483 (16.9), 308 (52.0), 273 (46.7)
[RuL ⁴][PF ₆] ₂	488 (29.8), 311 (68.3), 281 (sh, 77.0), 276 (78.8), 230 (97.5)
[RuL ⁵][PF ₆] ₂	488 (27.2), 310 (69.0), 281 (69.2), 276 (70.6)
[RuL ⁶][PF ₆] ₂	490 (28.5), 312 (63.4), 283 (62.0), 277 (61.6), 205 (sh, 120.3)
[Ru(terpy)L ⁴][PF ₆] ₂	482 (26.0), 309 (79.7), 280 (sh, 58.3), 273 (64.2), 229 (76.7)
[Ru(terpy)L ⁵][PF ₆] ₂ ·2H ₂ O	482 (22.7), 309 (71.4), 281 (sh, 48.9), 273 (54.5)
[Ru(terpy)L ⁶][PF ₆] ₂ ·2H ₂ O	483 (26.1), 309 (78.8), 280 (sh, 56.6), 273 (61.3)

^a $\lambda_{\text{max}}/\text{nm}$ ($10^{-3}\epsilon/\text{M}^{-1}\text{cm}^{-1}$) data from 10^{-5}M solutions in MeOH. ^b $\lambda_{\text{max}}/\text{nm}$ ($10^{-3}\epsilon/\text{M}^{-1}\text{cm}^{-1}$) data from 10^{-2}M solutions in acetone.

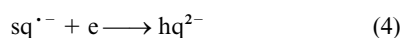
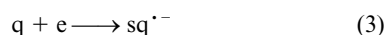
irreversible oxidation at +0.63 V was observed for L². Coulometry showed that two electrons per molecule were consumed and allows assignment of the process as the expected two-electron, two-proton oxidation of the hydroquinonyl (H₂hq) substituent to a quinonyl (q) substituent, *i.e.* equation (1).³⁰ A coupled



cathodic peak in the reverse positive scan at -0.45 V was observed for the reverse process, equation (2). For comparison,



in the same solvent system oxidation of 1,4-hydroquinone occurs at +0.67 V with a coupled cathodic peak at -0.26 V in the reverse scan for the reverse process; these processes are irreversible in aprotic solvents because the release and uptake of protons causes changes in the local pH at the electrode. The reversible couple at -0.76 V and the quasi-reversible couple at -1.29 V [$i_{\text{pa}}/i_{\text{pc}} \approx 1.0$ but $\Delta E_{\text{p}} = 150\text{ mV}$ compared with ΔE_{p} (ferrocenium-ferrocene) = 73 mV] are attributed to the quinone-semiquinone anion (q-sq⁻) and semiquinone anion-hydroquinone dianion (sq⁻-hq²⁻) couples respectively, equations (3) and (4) (for comparison, under the same

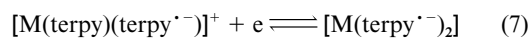
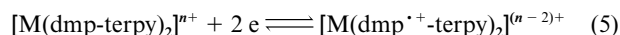


conditions 1,4-benzoquinone shows a reversible q-sq⁻ couple at -0.88 V and a quasi-reversible sq⁻-hq²⁻ couple at -1.75 V). The positive shift of the quinone-centred couples for L³ relative to 1,4-benzoquinone is consistent with the terpyridyl

group acting as an electron acceptor. There was no evidence for the terpy-terpy⁻ couple to more negative potentials before the cathodic solvent discharge.

Complexes. The electrochemical response for each complex is a combination of the processes expected for the [M(terpy)₂]ⁿ⁺ core and for the aryl ether, aryl ester, hydroquinonyl or quinonyl substituents. Data are summarized in Table 5.

(a) [M(terpy)₂]ⁿ⁺ core-centred processes. Fig. 6 shows representative cyclic voltammograms for the complexes of dimethoxyphenyl-substituted L¹ (dmp-terpy). These all show a quasi-reversible two-electron couple for oxidation of the two non-interacting dimethoxyphenyl (dmp) groups at $\approx +1.1\text{ V}$, equation (5),³⁰ and those of the complexes of Mn^{II}, Fe^{II}, Ru^{II}



and Zn^{II} show two reversible one-electron couples for successive reduction of the two co-ordinated terpyridyl centres at ≈ -1.6 and $\approx -1.8\text{ V}$ respectively, equations (6) and (7). Further electrochemical processes associated with the [M(terpy)₂]ⁿ⁺ cores are discussed by metal.

(i) **Zinc(II).** Only the aforementioned dimethoxyphenyl-centred oxidation and terpyridyl-centred reduction couples are observed, Fig. 6(h). No metal-centred redox processes are expected for the d¹⁰ zinc ion and none is observed.

(ii) **Manganese(II).** The only additional peaks were for the Mn^{III}-Mn^{II} couple which was observed as a broad, quasi-reversible one-electron process at +0.75 V ($\Delta E_{\text{p}} = 250\text{ mV}$ with

Table 5 Electrochemical data (in volts vs. ferrocenium–ferrocene) from cyclic voltammograms (scan rate = 100 mV s⁻¹) of complexes (≈1 mM) in acetonitrile–0.1 M tetrabutylammonium tetrafluoroborate at 25 °C

Complex	Ligand	M ^{III} –M ^{II}	M ^{II} –M ^I	terpy–terpy ^{•-}	Substituent processes
[MnL ₂][PF ₆] ₂	L ¹	+0.75 ^a		-1.53, -1.82	+1.01 ^b
	L ²	<i>c</i>		-1.53, -1.84	+0.72 (-0.37) ^d
	L ³	+0.8 ^a		-2.1 ^e	-0.78 ^{f,g}
[FeL ₂][BF ₄] ₂	L ¹	+0.69		-1.65, -1.74	+1.06 ^b
	L ²	+0.77		-1.60, -1.95	+0.59 (-0.34) ^d
	L ³	+0.77		-1.9 ^e	-0.61 ^{f,g}
[RuL(terpy)][PF ₆] ₂	L ¹	+0.86		-1.65, -1.92	+1.06 ^b
	L ²	+0.91		-1.72	+0.72 (-0.28) ^d
	L ³	+0.92		-1.66	-0.56, -1.38 ^h
[RuL ₂][PF ₆] ₂	L ¹	+0.84		-1.67, -1.91	+1.05 ^b
	L ²	+0.94		-1.64	+0.62 (-0.5) ^d
	L ³	+0.96		-1.82	-0.63 ^{f,g}
[CoL ₂][PF ₆] ₂	L ¹	-0.14	-1.17	-2.12	+1.06 ^b
	L ²	-0.15	-1.18	-2.05 ⁱ	+0.85 ^d
	L ³	-0.15	-1.32	-1.98 ^e	-1.11 ^f
[RhL ₂][PF ₆] ₃	L ¹	-1.06 (-0.68) ^{i,j}		-2.1 ⁱ	+1.06 ^b
	L ²	-1.07 (-0.69) ^{k,j}		-1.94 ⁱ	+0.70 (-0.52) ^d
	L ³	<i>ca.</i> -1.03 ^{e,j}			+0.50 ^{a,f,g}
[NiL ₂][PF ₆] ₂	L ¹			-1.59, -1.80	+1.02 ^b
	L ²			-1.58	+0.63 (-0.54) ^d
	L ³			-1.6 ^e	-0.61 ^{f,g}
[CuL ₂][PF ₆] ₂	L ¹	-0.72, ^{i,k} -0.94, ^{i,k}		<i>c</i>	+1.02 ^b
	L ²	-0.66, ⁱ -1.22 ⁱ		<i>c</i>	+0.82 (-0.46) ^d
	L ³	<i>c</i>		-2.2 ^e	-0.48 ^{f,g}
[ZnL ₂][PF ₆] ₂	L ¹			-1.66, -1.82	+1.01 ^b
	L ²			-1.62	+0.86 (-0.57) ^d
	L ³			-2.1 ^e	-0.77 ^{f,g}

^a Quasi-reversible couple. ^b dmp–dmp^{•+} couple. ^c Obscured by other process(es) or not observed. ^d Irreversible H₂hq substituent oxidation process; where observed, potentials for a coupled peak in the reverse scan are given in parentheses. ^e First peak of complicated reduction processes. ^f q–sq^{•-} couple. ^g Couple is not observed in the first scan and appears only after scanning through the complex reduction processes. ^h At negative potentials (*ca.* < -1.9 V). ⁱ Irreversible sq^{•-}–hq²⁻ process. ^j Irreversible process. ^k Rh^{III}–Rh^I process; potentials for a coupled peak in the reverse scan are given in parentheses. ^l Coupled to an absorption spike at -0.56 V in the reverse scan and merges to give a peak at *ca.* -1.19 V in the second and subsequent scans.

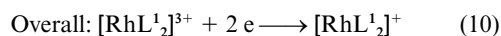
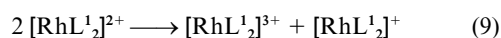
a scan rate of 50 mV s⁻¹), Fig. 6(a). The Mn^{III}–Mn^{II} couple for [Mn(terpy)₂]²⁺ at +0.84 V becomes poorly defined when the terpyridyl ligands are substituted by phenyl groups, *e.g.* [Mn(pterpy)₂]²⁺.^{8b-d}

(iii) *Iron(II)*. The reversible Fe^{III}–Fe^{II} couple at +0.69 V, Fig. 6(b), is the only extra process observed and expected. For comparison, the value for the Fe^{III}–Fe^{II} couple of [Fe(terpy)₂]²⁺ is +0.77 V.^{8e-g}

(iv) *Ruthenium(II)*. Likewise, [Ru(terpy)L]¹2⁺ and [RuL₂]²⁺, Fig. 6(c), exhibited reversible Ru^{III}–Ru^{II} couples at +0.86 and +0.84 V compared to +0.92 V for [Ru(terpy)₂]²⁺.^{8h}

(v) *Cobalt(II)*. In addition to the reversible, two-electron oxidation of the dimethoxyphenyl groups, [CoL₂]²⁺ displays reversible processes at -0.14, -1.17 and -2.12 V, Fig. 6(d), for the Co^{III}–Co^{II}, Co^{II}–Co^I, and (formal) Co^I–Co⁰ couples respectively (note, the latter could be either the Co^I–Co⁰ couple or the first terpyridyl-centred reduction couple). The corresponding couples for [Co(terpy)₂]²⁺ are observed at -0.13, -1.18 and -2.06 V.^{8e-g}

(vi) *Rhodium(III)*. The cyclic voltammograms of [RhL₂]³⁺ show the two-electron dimethoxyphenyl oxidation couple and an irreversible reduction process at -1.06 V with a daughter peak at -0.68 V after scan inversion, Fig. 6(e). Equal integrated peak currents for the reduction process and for the dimethoxyphenyl oxidation couple suggest that the reduction is a two-electron process. In scans extended to more negative potentials only broad indistinct processes are observed. Monomeric rhodium(II) complexes are unstable with respect to disproportionation to rhodium-(III) and -(I) species.³¹ It seems likely, therefore, that the electrochemically irreversible behaviour seen for reduction of [RhL₂]³⁺ arises because the rhodium(II) intermediate(s) disproportionate, equations (8) and (9). Overall this leads to a two-electron process, equation (10). Because



rhodium(I) complexes are typically four- or five-co-ordinate,³¹ a structural rearrangement may accompany reduction of [RhL₂]³⁺. Analogous reduction behaviour is observed for [Rh(bpy)₃]³⁺.³²

(vii) *Nickel(II)*. The complex [NiL₂]²⁺ showed a reversible one-electron reduction (by comparison with the two-electron oxidation of the two dimethoxyphenyl groups) at -1.59 V followed by two less distinct reduction couples at *ca.* -1.8 and -2.0 V, Fig. 6(f). The potential and peak current for the first reduction are consistent with the ligand-centred process, equation (6) (M = Ni). It is not possible definitively to assign the two other reductions. The complex [Ni(terpy)₂]²⁺ also shows three reduction processes, at -1.61, -1.84 and -2.28 V.^{8i,j} Analogous to our assignment, Prasad and Scaife^{8j} assign the reduction to the one-electron [Ni(terpy)₂]²⁺–[Ni(terpy)₂]^{•+} couple. In contrast Aihara *et al.*⁸ⁱ attribute the first process to two-electron reduction of the complex to give '[Ni(terpy)₂]' and the second to an electrochemically active species produced by ligand dissociation from '[Ni(terpy)₂]'. Prasad and Scaife^{8j} also observed a Ni^{III}–Ni^{II} couple at 1.26 V for [Ni(terpy)₂]²⁺. This couple was not seen for [NiL₂]²⁺ (L = L¹–L³; scans out to +1.6 V).

(viii) *Copper(II)*. Fig. 6(g) gives a typical cyclic voltammogram for [CuL₂]²⁺. The response at freshly polished platinum electrodes differed in the first and subsequent scans. The two reduction peaks observed at -0.72 and -0.94 V in the initial scan are attributed to the Cu^{II}–Cu^I and Cu^I–Cu⁰ reductions

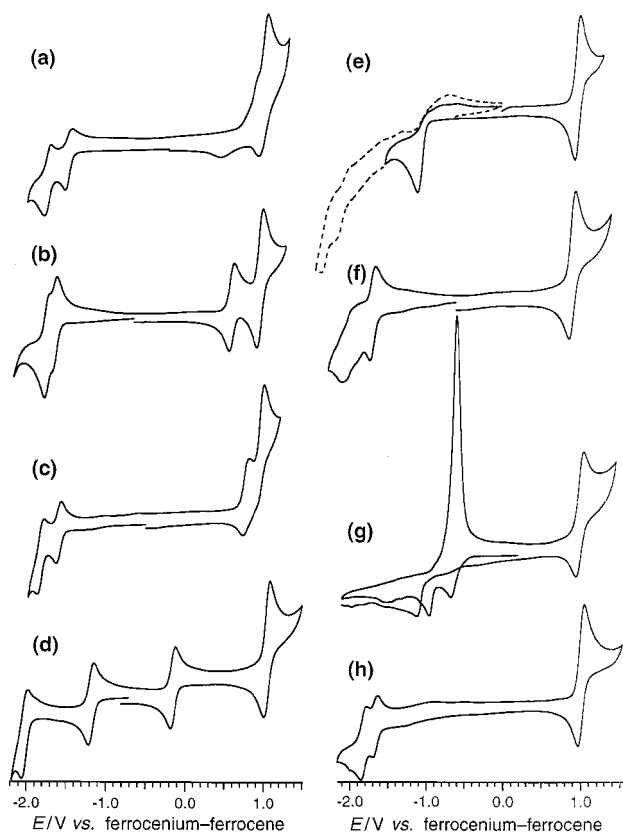


Fig. 6 Cyclic voltammograms in acetonitrile–0.1 M [NBu₄][PF₆] at a platinum-disc working electrode (scan rate = 100 mV s⁻¹) of the [ML₂]ⁿ⁺ complexes: M = Mn^{II} (a), Fe^{II} (b), Ru^{II} (c), Co^{II} (d), Rh^{III} (e), Ni^{II} (f), Cu^{II} (g) and Zn^{II} (h)

respectively and merge into a single peak at -1.19 V in subsequent scans. A stripping peak was seen at -0.56 V after scan inversion. Copper(II) polypyridyl complexes have Jahn–Teller distorted octahedral structures, *e.g.* the crystal structure of [CuL₂]²⁺ (see above). In contrast, polypyridyl copper(I) complexes typically are tetrahedral.³³ The electrochemically irreversible nature of the reduction couple(s) is ascribed to rearrangement concurrent with reduction, with the reduced species absorbing on the electrode and giving rise to the stripping peak in the reverse scan.^{8k}

(b) *Substituent-centred processes.* (i) *Complexes of L¹ and L⁶ (aryl ether substituents).* In addition to the above [M(terpy)₂]ⁿ⁺ core processes, cyclic voltammograms complexes of L¹ and L⁶ show a quasi-reversible oxidation of each aryl substituent to the radical cation, *e.g.* equation (5), at ≈+1.1 V for complexes of L¹ and ≈+1.0 V for complexes of L⁶ (*e.g.* see Fig. 6). The absence of splitting of the oxidation couple for the homoleptic complexes indicates that the two aryl ether substituents are electrochemically isolated.

(ii) *Complexes of L⁴ and L⁵ (aryl ester substituents).* Cyclic voltammograms of these complexes show a third reduction couple at ≈-2.1 V (negative of the two terpyridyl-centred reduction couples) for reduction of the ester-derivatized substituents in addition to the above [M(terpy)₂]ⁿ⁺ core processes. It is not fully reversible and gives rise to a small anodic peak at ≈-0.5 V in the reverse positive scan.

(iii) *Complexes of L² (hydroquinone substituents).* Cyclic voltammograms of these complexes show a broad anodic peak corresponding to the two-electron oxidation of each hydroquinone substituent to the quinone, equation (1), in the range +0.59 to +0.86 V, *e.g.* Fig. 7(a). Coulometry for [ZnL₂]²⁺ confirmed that the oxidation process consumed four electrons per molecule. The UV/VIS spectrum of the product was consistent with [ZnL₃]²⁺ having formed, equation (11) (M = Zn). The

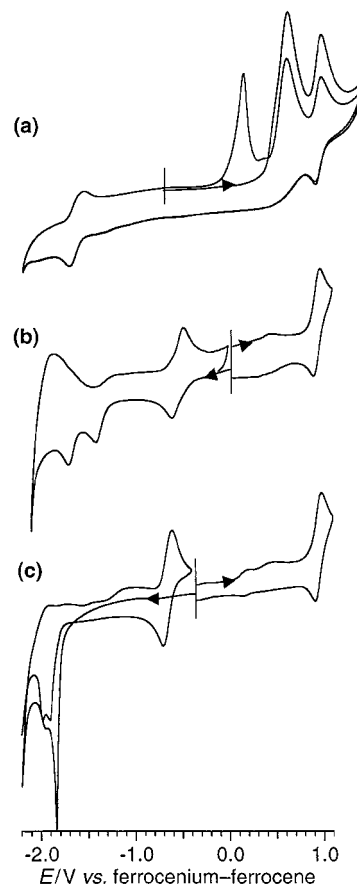
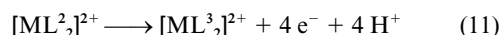


Fig. 7 Cyclic voltammograms in acetonitrile–0.1 M [NBu₄][PF₆] at freshly polished platinum-disc working electrodes (scan rate = 100 mV s⁻¹) of the complex cations: (a) [RuL₂]²⁺, (b) [Ru(terpy)₃]²⁺ and (c) [RuL₃]²⁺. The initial direction of each scan is indicated by an arrow



cyclic voltammograms also show the same metal-centred processes as those of the corresponding complexes of L¹ (see above), but the reductions of the [M(terpy)₂]ⁿ⁺ core are obscured or complicated by absorption and stripping phenomena. An anodic stripping peak between 0 to +0.4 V, *e.g.* see Fig. 7(a), was always observed in the reverse sweep after traversing the reductions of the [M(terpy)₂]ⁿ⁺ centres.

(iv) *Complexes of L³ (quinone substituents); aprotic conditions.* The cyclic voltammetric behaviour of the quinone-substituted complexes in aprotic solvents was complicated, *e.g.* Fig. 7(c). The cyclic voltammograms were dependent on the history and material of the working electrode (glassy carbon, gold and platinum electrodes were used) and on the scan range, and were different in the first and subsequent scans. Reproducible results were obtained with fresh, carefully deoxygenated solutions and newly polished platinum working electrodes and are reported here. The anticipated, reversible quinone–semiquinone (q–sq⁻) couple was seen in the first scan of [CoL₃]²⁺ (a two-electron process at ≈-1.11 V just prior to the one-electron Co^{II}–Co^I couple at -1.32 V) and of the heteroleptic complex [Ru(terpy)L³]²⁺ (a one-electron process at -0.56 V). Cyclic voltammograms of the latter complex, Fig. 7(b), also show a peak at -1.38 V for reduction of the semiquinone anion (sq⁻) to the hydroquinone dianion (hq²⁻). In contrast, the homoleptic complexes, [ML₃]²⁺ (M = Mn, Fe, Ru, Ni or Zn), revealed reversible q–sq⁻ couples at ≈-0.5 to -0.9 V (the exact potential depends on the transition-metal ion, Table 5), but with peak currents for a one-electron process and only in the second and subsequent scans after first sweeping through the complicated reduction processes at *ca.* -2.0 V (the latter processes are also seen for the

zinc complex and, therefore, are presumably ligand-centred), e.g. Fig. 7(c). However, controlled-potential electrolysis of $[\text{ZnL}^3]^{2+}$ at -1.0 V consumed 1.8 ± 0.1 Faraday mol^{-1} consistent with the expected addition of one electron per quinone group and conflicting with the 'apparent' one-electron currents observed in the cyclic voltammograms. The complicated nature of these at potentials negative of the $q\text{-sq}^{\cdot-}$ couples precludes assignment of the $sq^{\cdot-}\text{-hq}^{2-}$ couples. For the complexes of Fe^{II} and Ru^{II} the $q\text{-sq}^{\cdot-}$ couple became irreversible when the scan range was extended to include the $\text{M}^{\text{III}}\text{-M}^{\text{II}}$ couple. Similar scan-range-dependent reversibility has been observed for the ferrocenium-ferrocene couple in iron(II) complexes of ferrocenyl-substituted terpyridines.^{3n-q}

The voltammetric behaviour of the complexes of L^3 is not fully understood. Slow, rate-limiting heterogeneous charge transfer for the $q\text{-sq}^{\cdot-}$ couples would reconcile the apparently contrary observations of one-electron peak currents on the CV timescale and the consumption of two-electrons per molecule on the longer bulk electrolysis timescale, but is inconsistent with the reversible (Nernstian) peak-to-peak separations for these couples. The time-dependent nature of the cyclic voltammograms, and of the $q\text{-sq}^{\cdot-}$ couples in particular, and their dependence on electrode material and conditioning (including changes to the electrode surface due to scanning over different potential ranges) are more akin to the behaviour observed in the solution voltammetry of many redox proteins³⁴ where fast electron transfer occurs but only at selective microscopic sites on the electrode surface leading to radial diffusion and sigmoidally-shaped voltammograms when the concentration of sites is low (or no peaks in the limit of no sites) and to linear diffusion and 'normal' voltammetric peak shapes when the density of sites is increased sufficiently for overlap of the diffusion layers.

Protic conditions. It has already been seen that complexes of L^3 are obtained by chemical or electrochemical oxidation of the corresponding L^2 complex. The electrochemical interconversion between the complexes $[\text{ML}_2]^{2+}$ ($\text{M} = \text{Fe}, \text{Ru}$ or Zn ; $\text{L} = \text{L}^2$ or L^3) was investigated in acetonitrile— 0.1 M $[\text{NBu}_4][\text{PF}_6]$ with an excess of pyridinium toluene-*p*-sulfonate (ca. 0.03 M) added. Under these protic conditions, the cyclic voltammograms of the $[\text{ML}_2]^{2+}$ complexes became analogous to those of the $[\text{ML}_2]^{2+}$ complexes showing a broad reduction peak at ca. -0.6 V coupled to a peak in the reverse positive scan at ca. $+0.5$ V. Bulk electrolyses indicated that reduction of $[\text{ML}_2]^{2+}$ ($\text{M} = \text{Fe}$ or Zn) consumed four electrons per molecule of complex and the UV/VIS spectra of the reduction products were identical with those of the respective $[\text{ML}_2]^{2+}$ complexes. This suggests that $[\text{ML}_2]^{2+}$ and $[\text{ML}_3]^{2+}$ are interconverted by electrochemical oxidation and reduction, respectively, i.e. equation (11) is reversible under these protic conditions.

Conclusion

Terpyridyl ligands with redox-active dimethoxyphenyl, hydroquinonyl and quinonyl pendants and their complexes are easily prepared. Model derivatization reactions of the hydroquinonyl-substituted complexes $[\text{RuL}^2]^{2+}$ and $[\text{Ru}(\text{terpy})\text{L}^2]^{2+}$ suggest that complexes of L^2 are potentially useful as building blocks for the construction of multicomponent inorganic systems held together by ester or ether linkages. All of the complexes are electrochemically active and display characteristic $[\text{M}(\text{terpy})_2]^{n+}$ core- and 4'-substituent-centred redox processes; the electrochemical interconversion of the hydroquinonyl-substituted $[\text{ML}_2]^{2+}$ and quinonyl-substituted $[\text{ML}_3]^{2+}$ complexes is reversible in the presence of weak acid. Notably the metal centres in complexes of L^2 and L^3 can display different physical properties. For example, the complexes $[\text{CoL}_2]^{2+}$ ($\text{L} = \text{L}^2$ or L^3) are stable, can be interconverted either chemically or electrochemically, and display significantly different magnetic properties.

Experimental

General experimental methods and a description of electrochemical and spectroscopic instrumentation and techniques, apart from details of luminescence measurements, were given in full previously.^{3m} Steady-state luminescence measurements were made at room temperature (≈ 298 K) on ≈ 1 mM solutions of the complexes in de-oxygenated acetonitrile placed in $1 \times 1 \times 4$ cm³ polished quartz cuvettes using a Perkin-Elmer MPF-44B fluorescence spectrophotometer with a MacLab/8 AD interface to a Macintosh computer for data capture, storage and presentation. Excitation using a xenon lamp was at 300 or 490 nm and scans were recorded from 550 to 800 nm.

Preparations

3-(2,5-Dimethoxyphenyl)-1,5-bis(2-pyridyl)pentane-1,5-dione. 2,5-Dimethoxybenzaldehyde (1.0 g, 6.0 mmol) was dissolved in ethanol (100 cm³) and sodium hydroxide (1.0 g) in water (30 cm³) added. 2-Acetylpyridine (1.7 cm³, 13.0 mmol) was added dropwise and the solution stirred at room temperature for 40 h. The solvent was removed *in vacuo*, water (70 cm³) added to the residue and the mixture extracted with dichloromethane (3×50 cm³). The extract was concentrated and purified by flash chromatography (silica; dichloromethane as the eluent). A colourless band, which eluted after a yellow band, was collected, concentrated and recrystallized from diethyl ether to give clear crystals of the product (0.59 g, 25%). M.p. 97–99 °C (Found: C, 71.08; H, 5.88; N, 7.25. Calc. for $\text{C}_{23}\text{H}_{22}\text{N}_2\text{O}_4$: C, 70.77; H, 5.64; N, 7.18%). EI mass spectrum: m/z 390(M^+). ¹H NMR (CDCl_3): δ 8.62 (d, 2 H, $J = 4.6$, H⁶ of $\text{C}_5\text{H}_4\text{N}$), 7.95 (d, 2 H, $J = 7.9$, H³ of $\text{C}_5\text{H}_4\text{N}$), 7.77 (td, 2 H, $J = 7.6$, 1.8, H⁴ of $\text{C}_5\text{H}_4\text{N}$), 7.41 (ddd, 2 H, $J = 7.5$, 4.7, 1.3, H⁵ of $\text{C}_5\text{H}_4\text{N}$), 6.85 (d, 1 H, $J = 3.1$, H⁶ of dmp), 6.73 (d, 1 H, $J = 8.7$, H³ of dmp), 6.63 (dd, 1 H, $J = 8.7$, 3.1, H⁴ of dmp), 4.38 (q, 1 H, $J = 7.2$ Hz, CH), 3.73 (s, 3 H, MeO), 3.71 (m, 4 H, CH₂) and 3.68 (s, 3 H, MeO). ¹³C NMR (CDCl_3): δ 200.29, 153.53, 153.33, 151.49, 148.68, 136.61, 133.49, 126.74, 121.63, 114.64, 111.71, 111.29, 55.90, 55.48, 42.33 and 31.21. IR (Nujol mull): 1765s, 1620w, 1585m, 1496w, 1484m, 1355m, 1328w, 1317w, 1283m, 1260w, 1227s, 1174w, 1150w, 1127w, 1083w, 1056m, 1040w, 1028w, 995s, 982w, 974w, 869w, 795m, 777m, 749m, 710w and 691m cm⁻¹. UV/VIS (MeOH); $\lambda_{\text{max}}/\text{nm}$ ($10^{-3}\epsilon/\text{M}^{-1}\text{cm}^{-1}$) 270 (10.0) and 220 (sh, 27.0).

4'-(2,5-Dimethoxyphenyl)-2,2':6',2''-terpyridine (L^1). Method 1. 3-(2,5-Dimethoxyphenyl)-1,5-bis(2-pyridyl)pentane-1,5-dione (0.50 g, 1.3 mmol) and ammonium acetate (5.0 g) were heated at reflux for 4 h in ethanol (100 cm³). The solvent was removed *in vacuo* and water (200 cm³) added to the resulting brown oil. The mixture was extracted with dichloromethane (4×100 cm³), concentrated and purified by flash chromatography (silica; dichloromethane eluent). The broad light yellow band yielded a light yellow oil. Recrystallization of the oil from diethyl ether gave the product (0.35 g, 75%). M.p. 119–121 °C (Found: C, 75.15; H, 5.48; N, 11.12. Calc. for $\text{C}_{23}\text{H}_{19}\text{N}_3\text{O}_2$: C, 74.80; H, 5.15; N, 11.38%). EI mass spectrum: 369(M^+). 500 MHz ¹H NMR (CDCl_3): δ 8.69 (dq, 2 H, $J = 4.9$, 0.9, H⁶), 8.66 (dd, 2 H, $J = 7.9$, 1.1, H³), 8.64 (s, 2 H, H³), 7.87 (td, 2 H, $J = 7.7$, 1.8, H⁴), 7.30 (ddd, 2 H, $J = 7.7$, 4.8, 1.2, H⁵), 7.10 (dd, 1 H, $J = 2.6$, 0.7, H₁), 6.93 (dd, 1 H, $J = 9.0$, 0.7, H₂), 6.91 (dd, 1 H, $J = 8.9$, 2.8 Hz, H₂), 3.81 (s, 3 H, MeO) and 3.78 (s, 3 H, MeO). ¹³C NMR (CDCl_3): δ 156.38, 155.17, 153.69, 150.88, 149.02, 148.35, 136.70, 129.13, 123.55, 121.66, 121.26, 116.19, 114.68, 112.61, 56.30 and 55.84. IR (Nujol mull): 1600w, 1587s, 1568m, 1546m, 1500m, 1415w, 1302w, 1279m, 1267w, 1244m, 1226m, 1207m, 1187w, 1131w, 1070w, 1054m, 1042m, 1037m, 1020w, 990w, 920w, 900w, 880w, 855w, 817m, 790m, 778w, 745m and 729s cm⁻¹. UV/VIS (MeOH); $\lambda_{\text{max}}/\text{nm}$ ($10^{-3}\epsilon/\text{M}^{-1}\text{cm}^{-1}$) 338 (sh, 7.3), 319 (sh, 11.5), 283 (24.7), 278 (25.0) and 239.0 (30.8).

Method 2. 2,5-Dimethoxybenzaldehyde (9.25 g, 56 mmol), 2-acetylpyridine (14.5 cm³, 112 mmol), ammonium acetate (65 g, 0.84 mol) and acetamide (100 g, 1.7 mol) were heated at reflux for 2 h at 180 °C. The solution was allowed to cool and then sodium hydroxide (50 g) in water (120 cm³) was added and the mixture heated at reflux for 2 h. After cooling the mixture was decanted and the oily solid washed with water (3 × 200 cm³). The sludge was dissolved in the minimum volume of glacial acetic acid, concentrated hydrobromic acid (7 cm³) was added and the solution allowed to stand at room temperature for 16 h. The yellow precipitate was filtered off and placed in a beaker with water (300 cm³) and sodium hydrogencarbonate added until the solution was basic. The solid was extracted into chloroform, concentrated and purified by flash chromatography (silica; chloroform as the eluent). The broad gold band (fraction 3) was collected, concentrated and the light yellow oil dissolved in a small volume of diethyl ether from which it precipitated upon standing (8.26 g, 40%). M.p., UV/VIS and NMR spectroscopic data identical with those of the sample from the preceding preparation.

4'-(2,5-Dihydroxyphenyl)-2,2':6',2''-terpyridine (L²). Compound L¹ (0.46 g, 1.25 mmol) was heated at reflux in 48% hydrobromic acid (50 cm³) under nitrogen for 4 h. The solvent was distilled from the reaction mixture until solid began to precipitate. The reaction mixture was then cooled and solid NaHCO₃ added until the mixture was basic. The resulting yellow solid was collected by filtration, washed with water and recrystallized from ethanol to produce a light yellow powder (0.30 g, 70%). M.p. 245 °C (decomp.) (Found: C, 72.92; H, 4.63; N, 11.85. Calc. for C₂₁H₁₅N₃O₂·0.5H₂O: C, 72.21; H, 4.58; N, 12.03%). EI mass spectrum: 341(M⁺). ¹H NMR [(CD₃)₂SO]: δ 9.25 (br s, OH), 9.06 (br s, OH), 8.73 (d, 2 H, J = 4.1, H⁶), 8.70 (s, 2 H, H³), 8.66 (d, 2 H, J = 8.0, H³), 8.02 (td, 2 H, J = 7.7, 1.8, H⁴), 7.50 (br t, 2 H, J = 6.3, H⁵), 6.95 (d, 1 H, J = 2.8, H_f), 6.87 (d, 1 H, J = 8.7, H_e) and 6.74 (dd, 1 H, J = 8.6 Hz, 2.8, H_d). ¹³C NMR [(CD₃)₂SO]: δ 155.47, 154.93, 150.56, 149.46, 148.53, 147.58, 137.53, 125.23, 124.46, 120.94, 120.72, 117.64, 117.30 and 115.83. IR (Nujol mull): 3110w, 1610w, 1595s, 1570m, 1550m, 1510m, 1400m, 1320m, 1290m, 1279w, 1268w, 1254w, 1236w, 1205m, 1125w, 1080w, 1055w, 1040w, 1004w, 992w, 935w, 895w, 860w, 845w, 803w, 790w and 742w cm⁻¹. UV/VIS (MeOH): λ_{max}/nm (10⁻³ε/M⁻¹ cm⁻¹) 319 (10.0), 284 (22.1), 279 (21.9), 242 (23.4) and 205 (33.6).

4'-(1,4-Quinonyl)-2,2':6',2''-terpyridine (L³). The compound ddq (72 mg, 0.32 mmol) was added to L² (100 mg, 0.29 mmol) dissolved in acetone (25 cm³) and the solution stirred for 4 h. A yellow solid precipitated which was collected, washed well with diethyl ether and recrystallized from methanol to afford a bright yellow powder (54 mg, 55%). M.p. 226 °C (decomp.) (Found: C, 72.70; H, 4.12; N, 11.69. Calc. for C₂₁H₁₃N₃O₂·0.5H₂O: C, 72.41; H, 4.02; N, 12.07%). EI mass spectrum: 339(M⁺). ¹H NMR (CDCl₃): δ 8.70 (d, 2 H, J = 4.6, H⁶), 8.64 (d, 2 H, J = 8.0, H³), 8.55 (s, 2 H, H³), 7.88 (td, 2 H, J = 7.7, 1.8, H⁴), 7.36 (ddd, 2 H, J = 7.5, 4.9, 1.0, H⁵), 7.13 (d, 1 H, J = 2.3, H_f), 6.94 (d, 1 H, J = 10.3, H_e) and 6.88 (dd, 1 H, J = 10.2, 2.7 Hz, H_d). ¹³C NMR (CDCl₃): δ 187.09, 185.50, 155.90, 155.55, 149.24, 144.47, 142.26, 137.02, 136.92, 136.46, 133.98, 124.09, 121.32 and 120.72. IR (Nujol mull): 1665s, 1592w, 1578s, 1562w, 1540w, 1312w, 1292w, 1275m, 1148w, 1112w, 1085w, 1035w, 982w, 900w, 890m, 820w, 792w, 775w and 740w cm⁻¹. UV/VIS (MeOH): λ_{max}/nm (10⁻³ε/M⁻¹ cm⁻¹) 340 (sh, 6.2), 278 (24.4) and 246 (26.1).

General method for [ML₂][PF₆]₂ (M = Co, Cu, Mn, Ni or Zn). The appropriate metal acetate or chloride salt (0.29 mmol) was added to a solution of L¹ (200 mg, 0.59 mmol) in hot methanol (60 cm³). The mixture heated at reflux for 15 min. Excess of [NH₄][PF₆] was added and the solution refluxed for

5 min. Upon cooling a precipitate formed which was filtered off and washed with diethyl ether. Recrystallization from methanol afforded the products as microcrystalline solids.

[FeL₂][BF₄]₂. Compound L¹ (150 mg, 0.41 mmol) was dissolved in methanol (60 cm³) at reflux. [Fe(H₂O)₆][BF₄]₂ (67 mg, 0.20 mmol) in water (10 cm³) added dropwise, and the mixture heated at reflux for 15 min. Upon cooling a precipitate formed which was filtered off and washed with diethyl ether. Recrystallization from methanol afforded a purple microcrystalline solid (170 mg, 88%).

[RhL₂][PF₆]₃. Compound L¹ (120 mg, 0.33 mmol) and RhCl₃·3H₂O (42 mg, 0.16 mmol) were heated at reflux in methanol (40 cm³) containing *N*-ethylmorpholine (0.5 cm³) for 90 min. Excess of [NH₄][PF₆] in water (10 cm³) was added and the solution heated at reflux for 10 min. After cooling the solid was collected by filtration and recrystallized from acetone-methanol (1 : 1) to give the yellow microcrystalline product (145 mg, 70%).

[RuL₂][PF₆]₂. Compound L¹ (158 mg, 0.43 mmol) in methanol (60 cm³) was added to [Ru(dmsO)₄Cl₂] (104 mg, 0.21 mmol) in water (25 cm³) and the mixture heated at reflux for 30 min. The solvent was removed *in vacuo* and the residue dissolved in the minimum volume of methanol and purified by gel permeation chromatography (Sephadex LH20; methanol eluent). The initial bright red band was collected and the product precipitated with the addition of excess of aqueous [NH₄][PF₆]. The solid was filtered off and washed with diethyl ether to give the bright red microcrystalline product (150 mg, 62%).

General methods for [ML₂][PF₆]_n. *Method 1* (*n* = 2; M = Co, Cu, Fe, Mn, Ni or Zn). Compound L² (150 mg, 0.44 mmol) was dissolved in methanol (250 cm³) at reflux and an acetate or chloride salt of the appropriate metal ion (0.2 mmol) added and the mixture heated at reflux for 15 min. Excess of [NH₄][PF₆] in water (30 cm³) was added and the solution heated at reflux for 5 min. The solution was allowed to cool and the resulting precipitate filtered off and recrystallized from methanol. Yields were in the range 70–90%.

Method 2 (*n* = 2; M = Co, Cu, Fe, Mn, Ni, Ru or Zn; *n* = 3, M = Rh). The complex [ML₂][PF₆]_n or [ML₂][BF₄]_n (typically 100 mg) was heated at reflux for 3 h in concentrated hydrobromic acid (25 cm³) under a nitrogen atmosphere. The solvent was distilled from the reaction mixture until solid began to precipitate. After cooling, solid NaHCO₃ was added until the solution was basic. The resulting precipitate was filtered off, washed well with water and then recrystallized from methanol in the presence of an excess of [NH₄][PF₆]. Yields were in the range 85–95%.

[RuL₂][PF₆]₂. (a) The complex [Ru(dmsO)₄Cl₂] (17 mg, 0.35 mmol) in water (10 cm³) was added dropwise to L² (240 mg, 0.71 mmol) dissolved in methanol (50 cm³) and the solution heated at reflux for 30 min. The solvent was removed *in vacuo* and the residue dissolved in the minimum volume of methanol and purified by gel permeation chromatography (Sephadex LH20; methanol as the eluent). The initial bright red band was collected and the product precipitated by the addition of an excess of aqueous [NH₄][PF₆] to give a red powder (190 mg, 51%). (b) Method 2 gave the product in 78% yield. (c) The compound RuCl₃·3H₂O (120 mg, 0.53 mmol) and L² (370 mg, 1.08 mmol) were heated at reflux for 18 h in ethane-1,2-diol (60 cm³). Excess of [NH₄][PF₆] in water (60 cm³) was added and the solution heated for 10 min. After cooling the solution was filtered and the solid recrystallized from acetone-methanol (1 : 1) to give a red microcrystalline solid (375 mg, 66%).

General method for [ML₃][PF₆]_n (*n* = 2, M = Co, Cu, Fe, Mn, Ni, Ru or Zn; *n* = 3, M = Rh). The complex [ML₂][PF₆]₂ (5.0 mmol) and a slight excess of ddq (12.0 mmol) were dissolved in acetone (50 cm³, distilled from KMnO₄) and then from

anhydrous B_2O_3) and stirred at room temperature under nitrogen for 4 h. Dropwise addition of the solution to diethyl ether (200 cm^3) gave solids which were filtered off, washed with diethyl ether and then recrystallized from either acetone or methanol solution under a diethyl ether atmosphere. Yields were above 90%.

[Ru(terpy)L¹][PF₆]₂. The complex [Ru(terpy)Cl₃] (239 mg, 0.54 mmol) and L¹ (200 mg, 0.54 mmol) were heated at reflux in ethanol (200 cm^3), water (10 cm^3) and triethylamine (10 drops) for 14 h. After cooling the mixture was filtered through Celite and the solvent removed *in vacuo*. The remaining solid was dissolved in methanol and purified by gel permeation chromatography (Sephadex LH20; methanol as the eluent). The bright red central band was collected and precipitated by the addition of an excess of aqueous [NH₄][PF₆] to give a red microcrystalline solid (460 mg, 85%).

[Ru(terpy)L²][PF₆]₂. *Method 1.* The complex [Ru(terpy)Cl₃] (276 mg, 0.62 mmol) and L² (210 mg, 0.62 mmol) were heated at reflux under nitrogen for 18 h in ethanol (200 cm^3) and water (10 cm^3) with the addition of triethylamine (10 drops). The solvent was removed *in vacuo* and the residue dissolved in the minimum volume of methanol and purified by gel permeation chromatography (Sephadex LH20; methanol as the eluent). The bright red central band was collected and precipitated by the addition of an excess of aqueous [NH₄][PF₆] to give a red powder (0.27 g, 60%).

Method 2. The product was obtained in 85% yield using Method 2 for the preparation of homoleptic L² complexes.

[Ru(terpy)L³][PF₆]₂. This complex was obtained in 90% yield from [Ru(terpy)L²][PF₆]₂ using the general method described above for the preparation of [ML³]ⁿ⁺ complexes.

[RuL⁴]₂[PF₆]₂. The complex [RuL²]₂[PF₆]₂ (46 mg, 0.04 mmol) was dissolved in hot acetonitrile (35 cm^3) under a nitrogen atmosphere. Pyridine (2 cm^3) and an excess of benzoyl chloride (10 drops) were added and the solution heated at reflux for 16 h. The solvent was removed *in vacuo* and the residue dissolved in the minimum volume of acetonitrile and purified by flash chromatography [silica, acetonitrile–water–saturated KNO₃ (aq) (20:2:1) as eluent]. The large bright red band was collected and precipitated with the addition of an excess of [NH₄][PF₆] and then recrystallized from aqueous methanol to give a red microcrystalline solid (23 mg, 37%).

[RuL⁵]₂[PF₆]₂. The complex [RuL²]₂[PF₆]₂ (78 mg, 0.07 mmol) was dissolved in hot acetonitrile (35 cm^3) under a nitrogen atmosphere. Pyridine (2 cm^3) and an excess of propionyl chloride (10 drops) were added and the solution heated at reflux for 16 h. The solvent was removed *in vacuo* and the residue dissolved in the minimum volume of acetonitrile and purified by flash chromatography [silica, acetonitrile–water–saturated KNO₃ (aq) (20:2:1) as eluent]. The large bright red band was collected and precipitated with the addition of an excess of [NH₄][PF₆] and then recrystallized from methanol to give a red microcrystalline solid (58 mg, 64%).

[Ru(terpy)L⁴][PF₆]₂. The complex [Ru(terpy)L²][PF₆]₂ (46 mg, 0.04 mmol) was dissolved in hot acetonitrile (35 cm^3) under a nitrogen atmosphere. Pyridine (2 cm^3) and an excess of benzoyl chloride (10 drops) were added and the solution heated at reflux for 18 h. The solvent was removed *in vacuo* and the residue dissolved in the minimum volume of acetonitrile and purified by flash chromatography [silica, acetonitrile–water–saturated KNO₃ (aq) (20:2:1) as eluent]. The large bright red band was collected and precipitated with the addition of an excess of [NH₄][PF₆] and then recrystallized from acetone–methanol to give a red microcrystalline solid (38 mg, 44%).

[Ru(terpy)L⁵][PF₆]₂. The complex [Ru(terpy)L²][PF₆]₂ (78 mg, 0.07 mmol) was dissolved in hot acetonitrile (35 cm^3) under a nitrogen atmosphere. Pyridine (2 cm^3) and an excess of propionyl chloride (10 drops) were added and the solution heated at reflux for 16 h. The solvent was removed *in vacuo* and the residue dissolved in the minimum volume of acetonitrile and purified by flash chromatography [silica, acetonitrile–water–saturated KNO₃ (aq) (20:2:1) as eluent]. The prominent bright red band was collected and precipitated with the addition of an excess of [NH₄][PF₆] and then recrystallized from methanol to afford the red microcrystalline product (43 mg, 44%).

[RuL⁶]₂[PF₆]₂. The complex [RuL²]₂[PF₆]₂ (100 mg, 0.10 mmol) was dissolved in acetone (40 cm^3) at reflux under a nitrogen atmosphere. Excess of benzyl bromide (10 drops) and K₂CO₃ (50 mg, powdered with a mortar and pestle) were added and the solution heated at reflux for 16 h. The solution was filtered to remove the excess of K₂CO₃, the solvent was removed *in vacuo* and the residue dissolved in the minimum volume of acetonitrile and purified by flash chromatography [silica, acetonitrile–water–saturated KNO₃ (aq) (20:2:1) as eluent]. The major bright red band was collected. Precipitation with the addition of excess of [NH₄][PF₆] and recrystallization from methanol gave the red microcrystalline product (80 mg, 60%).

[Ru(terpy)L⁶][PF₆]₂. The complex [Ru(terpy)L²][PF₆]₂ (80 mg, 0.08 mmol) was dissolved in acetone (40 cm^3) at reflux under a nitrogen atmosphere. Excess of benzyl bromide (10 drops) and K₂CO₃ (50 mg, powdered with a mortar and pestle) were added and the solution heated at reflux for 16 h. The solution was filtered to remove the excess of K₂CO₃, and the solvent was removed *in vacuo* and the residue dissolved in the minimum volume of acetonitrile and purified by flash chromatography [silica, acetonitrile–water–saturated KNO₃ (aq) (20:2:1) as eluent]. The large bright red band was collected and precipitated with the addition of an excess of [NH₄][PF₆]. Recrystallization from methanol afforded the red microcrystalline product (52 mg, 55%).

X-Ray crystallography

Crystal data. C₂₃H₁₉N₃O₂, L¹, *M* 369.4, monoclinic, space group *C2/c*, *a* 24.161(4), *b* 9.188(1), *c* 21.330(3) Å, β 126.223(6)°, *U* 3820(1) Å³, *D_c* 1.28 g cm⁻³, *Z* 8, μ_{Cu} 6.35 cm⁻¹. Crystal size 0.15 × 0.15 × 0.35 mm, 2θ_{max} 140°, minimum and maximum transmission factors 0.80 and 0.89. The number of reflections was 2820 considered observed out of 3610 unique data, with *R_{merge}* 0.015 for 65 pairs of equivalent *0kl* reflections. Final residuals *R*, *R'* were 0.050, 0.078 for the observed data.

C₄₆H₃₈CuF₁₂N₆O₄P₂·CH₃OH, *M* 1124.4, triclinic, space group *P1̄*, *a* 10.041(5), *b* 14.918(7), *c* 16.566(8) Å, α 82.66(3), β 82.77(3), γ 85.08(3)°, *U* 2435(2) Å³, *D_c* 1.53 g cm⁻³, *Z* 2, μ_{Mo} 6.08 cm⁻¹. Crystal size 0.07 × 0.19 × 0.22 mm, 2θ_{max} 45°, minimum and maximum transmission factors 0.87 and 0.96. 4235 Observed reflections 4235 out of 6340 unique data, *R_{merge}* 0.019 for 290 pairs of equivalent *0kl* reflections. Final *R*, *R'* 0.063, 0.081 for the observed data.

Structure determinations. Reflection data were measured with an Enraf-Nonius CAD-4 diffractometer in θ–2θ scan mode at 298 K using nickel-filtered copper radiation (λ 1.5418 Å) for L¹ and graphite-monochromated molybdenum radiation (λ 0.7107 Å) for [CuL²]₂[PF₆]₂. Data were corrected for absorption using the analytical method of de Meulanaer and Tompa.³⁵ Reflections with *I* > 3σ(*I*) were considered observed. The structures were determined by direct phasing and Fourier methods. Hydrogen atoms were included in calculated positions and assigned thermal parameters equal to those of the atom to which they were bonded.

For L^1 , hydrogen atoms were included in calculated positions and assigned thermal parameters equal to those of the atom to which they were bonded. Positional and anisotropic thermal parameters for the non-hydrogen atoms were refined using full-matrix least squares.

For $[CuL_2][PF_6]_2$, the non-hydrogen atoms of the cation and the methanol were refined with individual positional and anisotropic thermal parameters. One of the anions, labelled B, was disordered, and so anion A and the two orientations of B were modelled as identical octahedra. Each orientation was defined by transformation to a local axis system of an idealized PF_6 octahedron described by a set of subsidiary coordinates. Refinement was accomplished by rotation and translation of these axis systems. Rigid constraints on the subsidiary coordinates maintained ideal geometry, and a common P–F distance was refined. The group thermal motions were described by rigid-body 15-parameter TLX models [T is the translation tensor, L the libration tensor and X the origin of libration (if defined)³⁶]. Refinement of the occupancies of the components of the disordered anion, constrained to total 1.0, converged to 0.55(1) and 0.45.

For both structures, reflection weights used were $1/\sigma^2(F_o)$, with $\sigma(F_o)$ being derived from $\sigma(I_o) = [\sigma^2(I_o) + (0.04I_o)^2]^{1/2}$. The weighted residual is defined as $R' = (\sum w\Delta^2/\sum wF_o^2)^{1/2}$. Atomic scattering factors and anomalous dispersion parameters were from ref. 37. Structure solutions were by MULTAN 80³⁸ and refinements used BLOCKLS, a local version of ORFLS,³⁹ for L^1 and RAELS⁴⁰ for $[CuL_2][PF_6]_2$. The program ORTEP II²² running on a Macintosh IIfx computer was used for the structural diagrams, and a DEC Alpha-AXP workstation for calculations.

CCDC reference number 186/898.

Acknowledgements

Support from the Australian Research Council is gratefully acknowledged.

References

- 1 J.-M. Lehn (Editor), *Comprehensive Supramolecular Chemistry*, Pergamon, Oxford, 1996, vols. 1–11.
- 2 (a) E. C. Constable, *Prog. Inorg. Chem.*, 1994, **42**, 67; (b) A. Harriman and J.-P. Sauvage, *Chem. Soc. Rev.*, 1996, 41; (c) A. Harriman and R. Ziessel, *Chem. Commun.*, 1996, 1707; (d) F. Barigelletti, L. Flamigni, J.-P. Collin and J.-P. Sauvage, *Chem. Commun.*, 1997, 333; (e) E. C. Constable, *Chem. Commun.*, 1997, 1073.
- 3 (a) C. Howard and M. D. Ward, *Angew. Chem., Int. Ed. Engl.*, 1992, **31**, 1028; (b) B. Whittle, N. S. Everest, C. Howard and M. D. Ward, *Inorg. Chem.*, 1995, **34**, 2025; (c) E. C. Constable and P. Harveson, *Chem. Commun.*, 1996, 33; (d) E. C. Constable and P. Harveson, *Inorg. Chim. Acta*, 1996, **252**, 9; (e) D. Armspach, M. Cattalini, E. C. Constable, C. E. Housecroft and D. Phillips, *Chem. Commun.*, 1996, 1823; (f) E. C. Constable and D. Phillips, *Chem. Commun.*, 1997, 827; (g) V. Marvaud and D. Astruc, *Chem. Commun.*, 1997, 773; (h) D. Armspach, E. C. Constable, F. Diederich, C. E. Housecroft and J.-F. Nierengarten, *Chem. Commun.*, 1997, 2009; (i) D. J. Cárdenas and J.-P. Sauvage, *Inorg. Chem.*, 1997, **36**, 2777; (j) E. C. Constable and A. M. W. Cargill Thompson, *J. Chem. Soc., Dalton Trans.*, 1992, 3467; (k) E. C. Constable and A. M. W. Cargill Thompson, *J. Chem. Soc., Dalton Trans.*, 1995, 1615; (l) G. D. Storrer and S. B. Colbran, *J. Chem. Soc., Dalton Trans.*, 1996, 2185; (m) G. D. Storrer, S. B. Colbran and D. C. Craig, *J. Chem. Soc., Dalton Trans.*, 1997, 3011; (n) J. C. Chambron, C. Coudret and J.-P. Sauvage, *New J. Chem.*, 1992, **16**, 361; (o) E. C. Constable, A. J. Edwards, R. Martínez-Mañez, P. R. Raithby and A. M. W. Cargill Thompson, *J. Chem. Soc., Dalton Trans.*, 1994, 645; (p) E. C. Constable, R. Martínez-Mañez, A. M. W. Cargill Thompson and J. V. Walker, *J. Chem. Soc., Dalton Trans.*, 1994, 1585; (q) E. C. Constable, A. J. Edwards, R. Martínez-Mañez and P. R. Raithby, *J. Chem. Soc., Dalton Trans.*, 1995, 3253; (r) E. C. Constable and R. A. Fallahpour, *J. Chem. Soc., Dalton Trans.*, 1996, 2389; (s) B. Whittle, S. R. Batten, J. C. Jeffery, L. H. Rees and M. D. Ward, *J. Chem. Soc., Dalton Trans.*, 1996, 4249.
- 4 J.-P. Sauvage, J.-P. Collin, J.-C. Chambron, S. Guillerez, C. Coudret, V. Balzani, F. Barigelletti, L. De Cola and L. Flamigni, *Chem. Rev.*, 1994, **94**, 993.
- 5 W. R. McWhinnie and J. D. Miller, *Adv. Inorg. Chem. Radiochem.*, 1969, **12**, 135; E. C. Constable, *Adv. Inorg. Chem. Radiochem.*, 1986, **30**, 69.
- 6 R. Hogg and R. G. Wilkins, *J. Chem. Soc.*, 1962, 341; P. M. Lutz, G. J. Long and W. A. Baker, *Inorg. Chem.*, 1969, **8**, 2529; L. Sacconi, *Pure Appl. Chem.*, 1971, **27**, 161; S. Kremer, W. Henke and D. Reinen, *Inorg. Chem.*, 1982, **21**, 3013 and refs. therein.
- 7 R. P. Thummel, V. Hegde and Y. Jahng, *Inorg. Chem.*, 1989, **28**, 3264; M. Beley, J.-P. Collin, J.-P. Sauvage, H. Sugihara, F. Heisel and A. Miehé, *J. Chem. Soc., Dalton Trans.*, 1991, 3157; C. R. Hecker, A. K. I. Gushurst and D. R. McMillin, *Inorg. Chem.*, 1991, **30**, 538; E. Amouyal, M. Mouallem-Bahout and G. Calzaferri, *J. Phys. Chem.*, 1991, **95**, 7641; E. Amouyal and M. Mouallem-Bahout, *J. Chem. Soc., Dalton Trans.*, 1992, 509; M. Maestri, N. Amaroli, V. Balzani, E. C. Constable and A. M. W. Cargill Thompson, *Inorg. Chem.*, 1995, **34**, 2759.
- 8 (a) M. C. Hughes and D. J. Macero, *Inorg. Chem.*, 1976, **15**, 2040; (b) M. M. Morrison and D. T. Sawyer, *Inorg. Chem.*, 1978, **17**, 333; (c) M. C. Hughes, D. J. Macero and J. M. Rao, *Inorg. Chim. Acta*, 1981, **49**, 241; (d) J. M. Rao, M. C. Hughes and D. J. Macero, *Inorg. Chim. Acta*, 1976, **18**, 127; (e) J. M. Rao, M. C. Hughes and D. J. Macero, *Inorg. Chim. Acta*, 1976, **16**, 231; (f) J. M. Rao, M. C. Hughes and D. J. Macero, *Inorg. Chim. Acta*, 1980, **41**, 221; (g) C. Arana, S. Yan, M. Keshavarz-K., K. T. Potts and H. D. Abruna, *Inorg. Chem.*, 1992, **31**, 3680; (h) E. C. Constable, A. M. W. Cargill Thompson, D. A. Tocher and M. A. M. Daniels, *New J. Chem.*, 1992, **16**, 855; (i) M. Aihara, H. Kishita and S. Misumi, *Bull. Chem. Soc. Jpn.*, 1975, **48**, 680; (j) R. Prasad and D. B. Scaife, *J. Electroanal. Chem. Interfacial Electrochem.*, 1977, **84**, 373; (k) A. L. Crumbliss and A. T. Poulos, *Inorg. Chem.*, 1975, **14**, 1529.
- 9 M. A. Fox and M. Channon (Editors), *Photoinduced Electron Transfer*, Elsevier, Amsterdam, 1988; M. R. Wasielewski, *Chem. Rev.*, 1992, **92**, 435; D. Gust, T. A. Moore and A. L. Moore, *Acc. Chem. Res.*, 1993, **26**, 198.
- 10 S. B. Colbran, D. C. Craig, W. M. Harrison and A. E. Grimley, *J. Organomet. Chem.*, 1991, **408**, C33; S. B. Sembiring, S. B. Colbran, D. C. Craig and A. D. Rae, *Inorg. Chem.*, 1995, **34**, 761; *J. Chem. Soc., Dalton Trans.*, 1995, 3731; W. M. Harrison, C. Saadeh and S. B. Colbran, *Organometallics*, 1997, **16**, 4254.
- 11 K. Schanze and K. Sauer, *J. Am. Chem. Soc.*, 1988, **110**, 1180; R. A. Berthon, S. B. Colbran and G. Moran, *Inorg. Chim. Acta*, 1993, **204**, 3; V. Gouille, A. Harriman and J. M. Lehn, *J. Chem. Soc., Chem. Commun.*, 1993, 1034; J. R. Schoonover, G. F. Strouse, P. Chen, W. D. Bates and T. J. Meyer, *Inorg. Chem.*, 1993, **32**, 2619; R. Wang, T. E. Keyes, R. Hage, R. H. Schmehl and J. G. Vos, *J. Chem. Soc., Chem. Commun.*, 1993, 1652; K. A. Opperman, S. L. Mecklenburg and T. J. Meyer, *Inorg. Chem.*, 1994, **33**, 5295.
- 12 P. Mitchell, *Nature (London)*, 1961, **191**, 144; J. Deisenhofer, O. Epp, K. Micki, R. Huber and H. Michel, *Nature (London)*, 1985, **318**, 618; J. Barber and B. Andersson, *Nature (London)*, 1994, **370**, 31; D. Xia, C.-A. Yu, H. Kim, J.-Z. Xia, A. M. Kachurin, L. Zhang, L. Yu and J. Deisenhofer, *Science*, 1997, **277**, 60.
- 13 D. G. Nicholls and S. J. Ferguson, *Bioenergetics 2*, Academic Press, New York, 1992.
- 14 G. D. Storrer, S. B. Colbran and D. B. Hibbert, *Inorg. Chim. Acta*, 1995, **239**, 1.
- 15 W. Spahni and G. Calzaferri, *Helv. Chim. Acta*, 1984, **67**, 450.
- 16 E. C. Constable, J. Lewis, M. C. Liptrot and P. R. Raithby, *Inorg. Chim. Acta*, 1990, **178**, 47.
- 17 J. S. Foos, S. M. Erker and L. M. Rembetsy, *J. Electrochem. Soc.*, 1986, **133**, 836; V. Le Berre, L. Angely, J. Simonet, G. Mousset and M. Bellec, *J. Electroanal. Chem. Interfacial Electrochem.*, 1987, **218**, 173; Y. Gache and J. Simonet, *J. Electroanal. Chem. Interfacial Electrochem.*, 1987, **218**, 173.
- 18 G. Allen and J. C. Bevington (Editors), *Comprehensive Polymer Science: The Synthesis, Characterization, Reactions & Applications of Polymers*, Pergamon, Oxford, 1989.
- 19 A. H. Crosby and R. E. Lutz, *J. Am. Chem. Soc.*, 1956, **78**, 1233.
- 20 E. P. Platnova, L. I. Polishchuk, Ya. I. Kurys' and V. D. Pokhodenko, *Elektrokhimiya*, 1990, **26**, 326; K. Kaleem, F. Chertok and S. Erhan, *Prog. Org. Coat.*, 1987, **15**, 63; K. Kaleem, F. Chertok and S. Erhan, *J. Polym. Sci., A: Polym. Chem.*, 1989, **27**, 865.
- 21 B. N. Figgis, E. S. Kucharski and A. H. White, *Aust. J. Chem.*, 1983, **36**, 1563; E. N. Maslen, C. L. Raston and A. H. White, *J. Chem. Soc., Dalton Trans.*, 1974, 1803; B. N. Figgis, E. S. Kucharski and A. H. White, *Aust. J. Chem.*, 1983, **36**, 1527; C. L. Raston and A. H. White, *J. Chem. Soc., Dalton Trans.*, 1976, 7; F. Tukasagawa, P. G. Yohannes and K. B. Mertes, *Inorg. Chim. Acta*, 1986, **114**, 165; W. Henke and S. Kremer, *Inorg. Chim. Acta*, 1982, **65**, L112; B. N.

- Figgis, E. S. Kucharski and A. H. White, *Aust. J. Chem.*, 1983, **36**, 1537.
- 22 C. K. Johnson, ORTEP II, Oak Ridge National Laboratory, Oak Ridge, TN, 1976.
- 23 R. Allmann, W. Henke and D. Reinen, *Inorg. Chem.*, 1978, **17**, 378.
- 24 D. F. Evans, *J. Chem. Soc.*, 1959, 2003.
- 25 See, for example, M. L. Boillot, C. Roux, J.-P. Audiere, A. Dausse and J. Zarembowitch, *Inorg. Chem.*, 1996, **35**, 3975 and refs. therein.
- 26 I. Bertini and C. Luchinat, *NMR of Paramagnetic Substances*, Elsevier, Amsterdam, 1996.
- 27 W. De W. Horrocks, *Inorg. Chem.*, 1970, **9**, 690.
- 28 T. Itoh, *Chem. Rev.*, 1995, **95**, 2351.
- 29 A. Zweig, W. G. Hodgson and W. H. Jura, *J. Am. Chem. Soc.*, 1964, **86**, 4124.
- 30 B. R. Eggins and J. Q. Chambers, *J. Electrochem. Soc.*, 1970, **117**, 186.
- 31 F. H. Jardine and P. S. Sheridan, *Comprehensive Coordination Chemistry*, ed. G. Wilkinson, Pergamon, Oxford, 1987, vol. 4, p. 901.
- 32 S.-F. Chan, M. Chou, T. Matsubara and N. Sutin, *J. Am. Chem. Soc.*, 1981, **103**, 369.
- 33 B. J. Hathaway, in *Comprehensive Coordination Chemistry*, ed. G. Wilkinson, Pergamon, Oxford, 1987, vol. 5, p. 553.
- 34 F. A. Armstrong, A. M. Bond, A. O. Hill, B. N. Oliver and I. S. M. Psalti, *J. Am. Chem. Soc.*, 1989, **111**, 9185; A. M. Bond, *Inorg. Chim. Acta*, 1994, **226**, 293.
- 35 J. De Meulenaer and H. Tompa, *Acta Crystallogr.*, 1965, **19**, 1014.
- 36 A. D. Rae, *Acta Crystallogr., Sect. A*, 1975, **31**, 560.
- 37 J. A. Ibers and W. C. Hamilton (Editors), *International Tables for X-Ray Crystallography*, Kynoch Press, Birmingham, 1974, vol. 4.
- 38 P. Main, MULTAN 80, University of York, 1980.
- 39 A. D. Rae, RAELS, A Comprehensive Constrained Least Squares Refinement Program, University of New South Wales, 1989.
- 40 W. R. Busing, K. O. Martin and H. A. Levy, ORFLS, Oak Ridge National Laboratory, Oak Ridge, TN, 1962.

Received 22nd December 1997; Paper 7/09117F